iScience

CellPress
OPEN ACCESS

Article

Piezo-mediated mechanosensation contributes to stabilizing copulation posture and reproductive success in *Drosophila* males

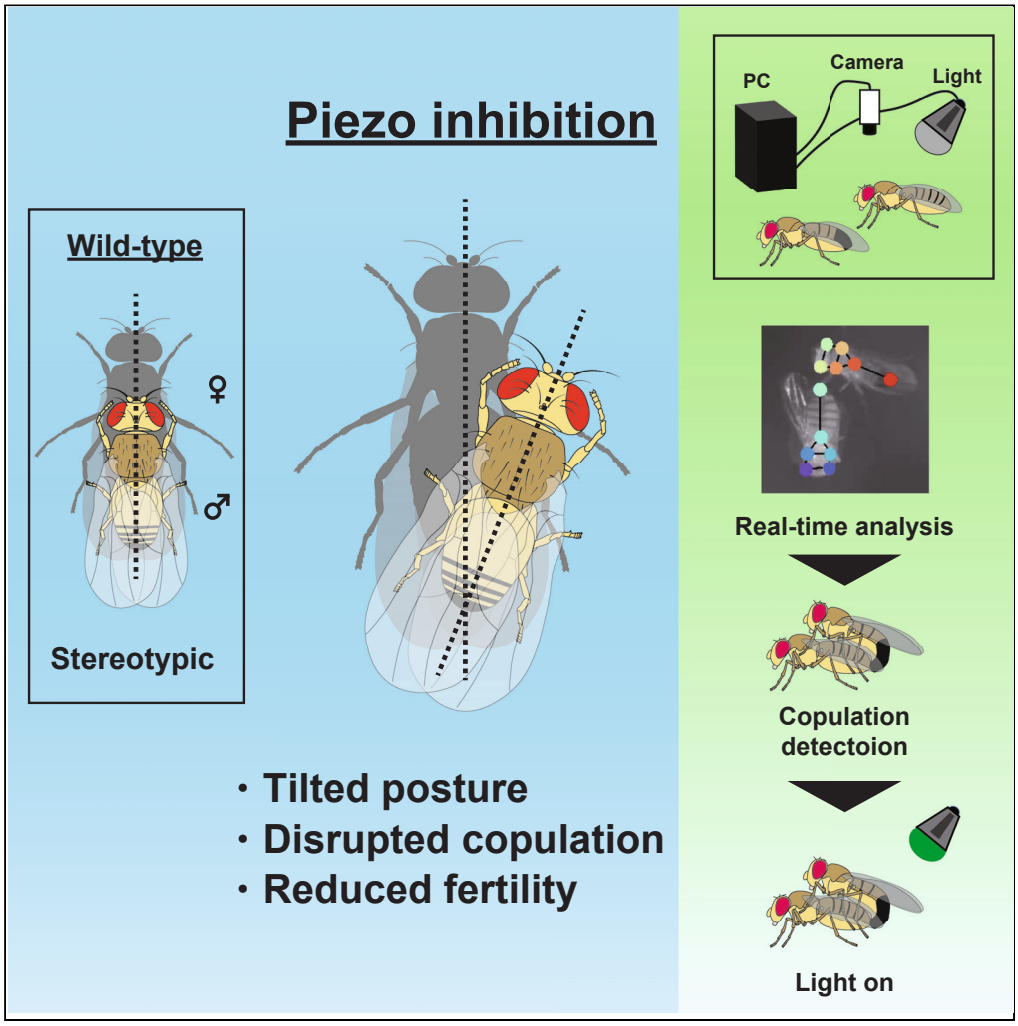

Hayato M. Yamanouchi, Ryoya Tanaka, Azusa Kamikouchi

tanaka.ryoya.z3@f.mail.nagoya-u.ac.jp (R.T.)
kamikouchi.azusa.r4@f.mail.nagoya-u.ac.jp (A.K.)

Highlights

Mechanosensation by *piezo* in male *Drosophila* promotes stabilized copulation

Disruption of *piezo* results in destabilized copulation posture and reduced offspring

Piezo is expressed in the mechanosensory bristle neurons of male genitalia

Yamanouchi et al., iScience 26, 106617
May 19, 2023 © 2023 The Author(s).
https://doi.org/10.1016/j.isci.2023.106617

iScience

CellPress
OPEN ACCESS

Article

Piezo-mediated mechanosensation contributes to stabilizing copulation posture and reproductive success in *Drosophila* males

Hayato M. Yamanouchi,[1] Ryoya Tanaka,[1,3,*] and Azusa Kamikouchi[1,2,3,4,*]

SUMMARY

In internal fertilization animals, reproductive success depends on maintaining copulation until gametes are transported from male to female. In *Drosophila melanogaster*, mechanosensation in males likely contributes to copulation maintenance, but its molecular underpinning remains to be identified. Here we show that the mechanosensory gene *piezo* and its' expressing neurons are responsible for copulation maintenance. An RNA-seq database search and subsequent mutant analysis revealed the importance of *piezo* for maintaining male copulation posture. *piezo-GAL4*-positive signals were found in the sensory neurons of male genitalia bristles, and optogenetic inhibition of *piezo*-expressing neurons in the posterior side of the male body during copulation destabilized posture and terminated copulation. Our findings suggest that the mechanosensory system of male genitalia through Piezo channels plays a key role in copulation maintenance and indicate that Piezo may increase male fitness during copulation in flies.

INTRODUCTION

In internally fertilizing animals, reproduction is dependent on prolonging copulation until gametes are transported from the male to the female reproductive organ. Copulation termination before gamete transport prevents females from becoming fertile.[1,2] During copulation, the male keeps coupling his genitalia to the female's genitalia by maintaining a specific copulation posture suggesting that maintaining copulation posture is important to maintain genital coupling.[3,4] The genitalia and abdominal structures of both males and females are adaptively tuned in a species-specific manner, like a lock and key, to maintain copulation posture.[4–6] Despite accumulating knowledge of morphological aspects of copulation posture maintenance, the neuronal and/or molecular mechanisms underlying it are largely unexplored. The fruit fly *Drosophila melanogaster* serves as a suitable model for such studies, as its mating behavior is easily quantified under laboratory conditions,[7] together with the availability of various genetic tools to manipulate gene expression and neural activity.[8,9]

Before starting copulation, male *D. melanogaster* display courtship behaviors toward a target female, including orientation, tapping, following, singing, licking, and attempted copulation.[10] When the male initiates courtship, females typically exhibit signatures of pre-mating rejection such as escaping and kicking.[11] However, as the male continues courtship, females gradually decrease locomotion and eventually accept copulation.[11] At the attempted copulation stage, a male bends his abdomen in an effort to couple his genitalia with that of the female, and if the female is sufficiently receptive, they will couple their genitalia to initiate copulation.[12,13] Following their genital coupling, the male mounts on the female and maintains his position.[14–16] The duration of copulation (i.e., genital coupling) is almost the same as that of the "male mounting on a female" period, during which the male maintains his copulation posture.[16–19] The male needs to continue this posture at least until he transfers sufficient sperm for fertile mating, which occurs about 8 min after copulation initiation.[1]

Regulation of copulation posture likely involves the interplay of the central and peripheral nervous systems, including the mechanosensory system of the male genitalia. The male genitalia are covered with sensory bristles, with sensory neurons projecting to the base.[20] Among these sensory bristles, a single pair of long mechanosensilla is known for its importance in determining copulation posture, as ablation

[1]Graduate School of Science, Nagoya University, Nagoya, Aichi 464-8602, Japan

[2]Institute of Transformative Bio-Molecules (WPI-ITbM), Nagoya University, Nagoya, Aichi 464-8602, Japan

[3]These authors contributed equally

[4]Lead contact

*Correspondence: tanaka.ryoya.z3@f.mail.nagoya-u.ac.jp (R.T.), kamikouchi.azusa.r4@f.mail.nagoya-u.ac.jp (A.K.)

https://doi.org/10.1016/j.isci.2023.106617

This is an open access article under the CC BY-NC-ND license (http://creativecommons.org/licenses/by-nc-nd/4.0/).

of a single one tends to tilt the posture of copulating males.[21] In the male abdominal ganglion, mechanosensory neurons at the sensory bristles of male genitalia have synaptic and functional connections to a sexually dimorphic motor circuit that mediates the motor sequence of initiating and terminating copulation.[17] The motor neurons in this circuit regulate the phallic and periphallic musculature, which regulates genital grasping of the female genitalia,[22] depending on mechanosensory inputs.[17] Inhibition of *fruitless* (*fru*) neurons in the male genitalia (including fru^{+} mechanosensory neurons) results in shorter copulation duration, raising the possibility that mechanosensory neurons of the male genitalia are involved in the regulation of copulation duration.[23] These previous studies together suggest that males receive mechanosensory information from females in copula via mechanosensory bristles of the genitalia, and use that information to maintain copulation until gametes are transported to the female. Which mechanosensory channels are expressed in these bristles and how they contribute to the maintenance of copulation, however, remains underexplored.

Several types of mechanosensory channels have been identified in *D. melanogaster*. Among them, *piezo*, *nompC*, *nanchung* (*nan*), and *inactive* (*iav*) are expressed in the sensory bristle neurons of *Drosophila*.[24] Functionally, NompC, Nanchung (Nan), and Inactive (Iav) are known as hearing genes; these three transient receptor potential (TRP) channels are expressed in the mechanosensory neurons within the fly ear and are involved in the auditory mechanotransduction.[25–27] In mechanosensory neurons of Johnston's organ (the sensory organ of the fly ear), Nan and Iav form heteromeric channels and are required for electrical signaling, possibly at the step of auditory mechanotransduction.[27,28] Mutations in *nompC* channels reduce the amplitude and sensitivity of sound-evoked nerve responses from the Johnston's organ, suggesting that NompC acts as a mechanical pre-amplifier in the fly ear.[29] In the larval body wall neurons, NompC senses gentle touch and regulates locomotion.[30,31]

Another mechanosensory channel, Piezo, is a *Drosophila* homolog of the mammalian Piezo channels.[32] It induces a mechanically activated current as is the case for its mammalian counterparts.[32–34] In adult *D. melanogaster*, Piezo channels are responsible for internal and external mechanosensation.[35–38] As part of its function as an internal sensor, Piezo channels detect the expansion and contraction of the crop, which contributes to the regulation of feeding behavior.[35–37] As an example of its role as an external sensor, Piezo expressed in the sensory neurons of the mechanosensory bristles at female genitalia and/or in neurons innervating the reproductive tract contributes to female mating experience.[38]

In this study, we explored the mechanosensory mechanisms underlying male copulation maintenance. To select candidate channels involved in the copulation maintenance of males, we utilized the single-cell transcriptome database of the entire adult fly.[39] We found *piezo* as a highly enriched mechanosensory gene in the neural clusters of the male body wall dataset, which includes the mechanosensory bristle cells of the male genitalia. We observed the copulation of *piezo* mutant ($Piezo^{KO}$) males and found their body axis tended to tilt during copulation, suggesting *piezo* is involved in copulation posture maintenance. In addition, wild-type females that copulated with $Piezo^{KO}$ males produced fewer offspring than those copulated with control males, indicating reduced male fitness. Molecular-genetic analysis showed that *piezo* was expressed in the mechanosensory bristle neurons in the male genitalia, which play important roles to maintain copulation. When *piezo*-expressing neurons on the posterior side were optogenetically suppressed during copulation, the copulation was disrupted and terminated. Taken together, our findings revealed a significant role of Piezo-mediated mechanosensation in copulation maintenance and reproductive success.

RESULTS

The *piezo* gene contributes to maintaining copulation posture

Mechanosensory bristles on the male external genitalia are important for maintaining male copulation postures.[21] Mechanoreception in the male genitalia during copulation, likely mediated by mechanosensory channels, thus possibly plays a significant role in male copulation posture. Previous studies have reported gene expression of mechanosensory channels *piezo*, *nompC*, *nanchung* (*nan*), and *inactive* (*iav*) in the sensory bristle neurons of *Drosophila*,[24] making them candidates for the molecular component involved in keeping the male copulation posture. To narrow down candidate mechanosensory channels that contribute to this process, we used a large-scale single-cell RNA-seq analysis platform, SCope.[39,40] Since no dataset of genital sensory neurons was available in SCope, we used the male's body wall data that potentially include the sensory neurons in the external genitalia.[39]

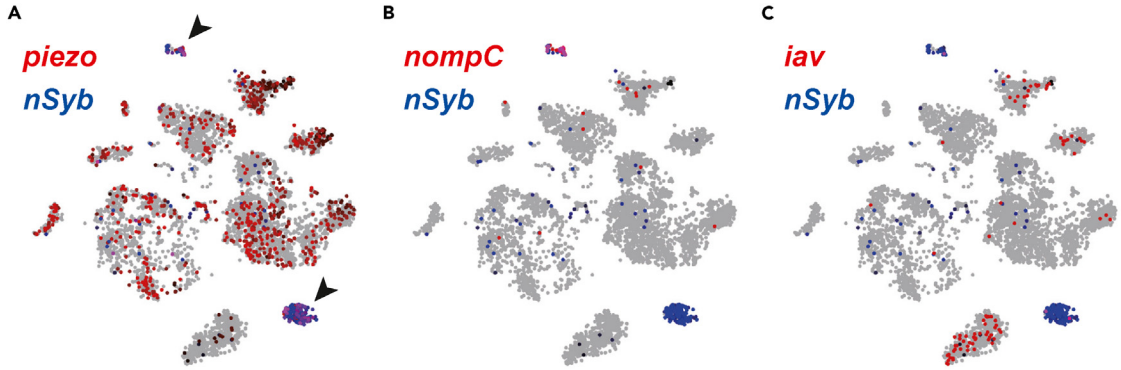

Figure 1. Abundant expression of *piezo* in the nervous system of the body wall

Expression profiles of *piezo* (A), *nompC* (B), and *iav* (C) genes in the body wall data of *Drosophila* males. Images from the single-nucleus transcriptome atlas database SCope[39] (http://scope.aertslab.org) are shown. The cells co-expressing the mechanosensory channel gene (red) and *nSyb* (blue) are colored in violet. *piezo* gene is abundantly expressed in the nervous system clusters[39] indicated by arrowheads (Top, peripheral nervous system cluster; Bottom, ventral nervous system cluster).

In the SCope database, the body wall data is annotated into cell types, such as the peripheral or ventral nervous system, fat body, and hemocyte[39] (Figure S1). Because previous studies suggested that males detect genital coupling via genital mechanosensory neurons during copulation,[17,23] we focused on neuronal clusters in this dataset which potentially include sensory neurons: the peripheral and ventral nervous system clusters. These two clusters abundantly expressed the *neuronal Synaptobrevin* (*nSyb*) gene, a marker of neuronal cells,[41] verifying their neuronal properties (Figure 1). In these two neuronal clusters, we detected the expression of three mechanosensory channels, *piezo*, *nompC*, and *iav* (but not *nan*), among which *piezo* was the most abundant (Figure 1). A previous study using male mice identified Piezo1 expression in the ejaculatory ducts and surrounding tissues, indicating that Piezo1-mediated mechanosensation is possibly involved in male ejaculatory function.[42] We thus focused on the *Drosophila piezo* gene in the following experiments.

The *piezo* gene encodes a component of a mechanosensory channel[36]. In females, mechanosensation by Piezo reduces receptivity after copulation.[38] However, the effect of Piezo on copulation in males remains underexplored, including its involvement in the copulation posture. In order to investigate the possible role of Piezo in copulation postures, we observed copulation behaviors of $Piezo^{KO}$ males paired with wild-type females. $Piezo^{KO}$ males actively courted females, and in most cases successfully started copulation, as judged by genital coupling between the male and female. However, although their genitalia kept coupled, the copulation postures of $Piezo^{KO}$ males were unstable; they often tilted during the entire copulation period when compared to the wild-type males (Figures 2A and 2B). This phenotype looked similar to the tilted copulation postures observed in wild-type males whose one of the genital long mechanosensilla was ablated.[21]

Using DeepLabCut, a machine-learning-based markerless animal pose estimation tool,[43] we quantified the postures of males throughout copulation events. The ratio of time in which the male engaged in tilted copulation (i.e., copulation angle, the angle between the body axes of two flies engaged in copulation, was $\geq$ 25°) was significantly larger in $Piezo^{KO}$ homozygous males than in control flies (Figures 2C and S2A–S2K). Furthermore, the copulation angle of $Piezo^{KO}$ homozygous males was indeed unstable when compared to that in control flies, as copulations of $Piezo^{KO}$ homozygous males fluctuated between tilted and stereotypic angles more frequently than those of control flies, resulting in a significantly larger variance of copulation angle (Figures 2B, 2D, and 2E).

The tilted copulation observed in $Piezo^{KO}$ homozygous males may be due to the rejection behavior of females in copula. Indeed, a prior study in *D. melanogaster* observed that the female kicks the male with her hind legs during copulation.[44] We examined if females coupled with $Piezo^{KO}$ homozygous males showed more intense kicking behavior than those with wild-type males. Contrary to our speculation, females kicked wild-type males as frequently as $Piezo^{KO}$ homozygous males (Figure S3A). This finding suggests that *piezo* mutation in males has no significant effect on female kicking behaviors during copulation. Another

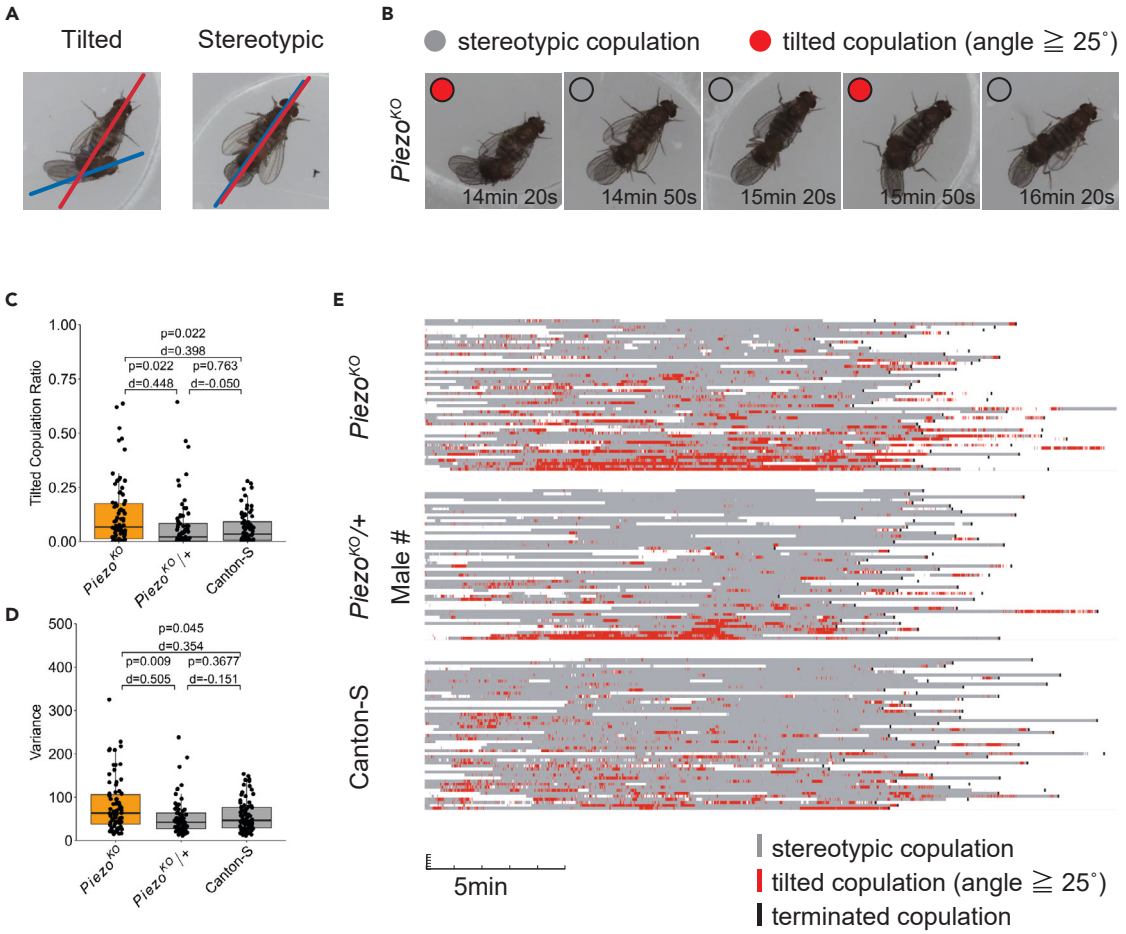

Figure 2. Piezo contributes to stabilizing copulation postures in males

(A) Top view of tilted or stereotypic copulation posture. The red and blue lines indicate the body axis of the female and male, respectively. The angle between the red and blue lines is larger in tilted copulation than in stereotypic copulation.

(B) Top view of *Piezo*^{KO} copulation posture. The circles show stereotypic copulation posture (gray) or tilted copulation posture (copulation angle ≥ 25°) (red).

(C) The ratio of time in which the male engaged in tilted copulation (copulation angle ≥ 25°) for *Piezo*^{KO}, *Piezo*^{KO}/+, and Canton-S males. The aligned rank transform one-way analysis of variance (ART one-way ANOVA) test corrected with the Benjamini-Hochberg method was used for statistical analysis. Boxplots display the medians (horizontal white line in each box) with 25th and 75th percentiles and whiskers denote 1.5x the interquartile range. Each point indicates individual data. p and d indicate the p value and Cohen's d effect size, respectively. The ratio of tilted copulation was calculated in individual pairs for which the tracking analysis in DeepLabCut was successfully performed for longer than 5 min in total. *Piezo*^{KO}, n = 75; *Piezo*^{KO}/+, n = 66; and Canton-S, n = 78.

(D) Variance of copulation angle for *Piezo*^{KO}, *Piezo*^{KO}/+, and Canton-S males. ART one-way ANOVA test corrected with the Benjamini-Hochberg method was used for statistical analysis. Boxplots display the medians (horizontal white line in each box) with 25th and 75th percentiles and whiskers denote 1.5x the interquartile range. Each point indicates individual data. p and d indicate the p value and Cohen's d effect size, respectively. The variance of tilted copulation was calculated in individual pairs for which the tracking analysis in DeepLabCut was successfully performed for longer than 5 min in total. *Piezo*^{KO}, n = 75; *Piezo*^{KO}/+, n = 66; and Canton-S, n = 78.

(E) Ethogram of male copulation posture for *Piezo*^{KO}, *Piezo*^{KO}/+, and Canton-S males. The horizontal and vertical axes represent the observation period and male individuals, respectively. The colored area shows the time of DeepLabCut analysis with stereotypic copulation (gray), tilted copulation (copulation angle ≥ 25°) (red), and copulation termination (black). For plotting the ethogram of each genotype, 50 pairs with longer tilted copulation than other pairs of the same genotype were selected. The individual pairs are sorted from top to bottom in order of the length of tilted copulation time.

possibility we speculated was that the *piezo* mutation might affect the ability of the male genitalia to capture the female's genitalia, which is required for successful copulation. We addressed this possibility by measuring the frequency of male genital touching before copulation (i.e., the male bending his abdomen and touching female genitalia before copulation initiation). Again, no significant difference was detected in this touching frequency between *Piezo*^{KO} homozygous males and wild-type males (Figure S3B). These results exclude the possibility that tilted copulation posture in *Piezo*^{KO} males was due to females' rejection

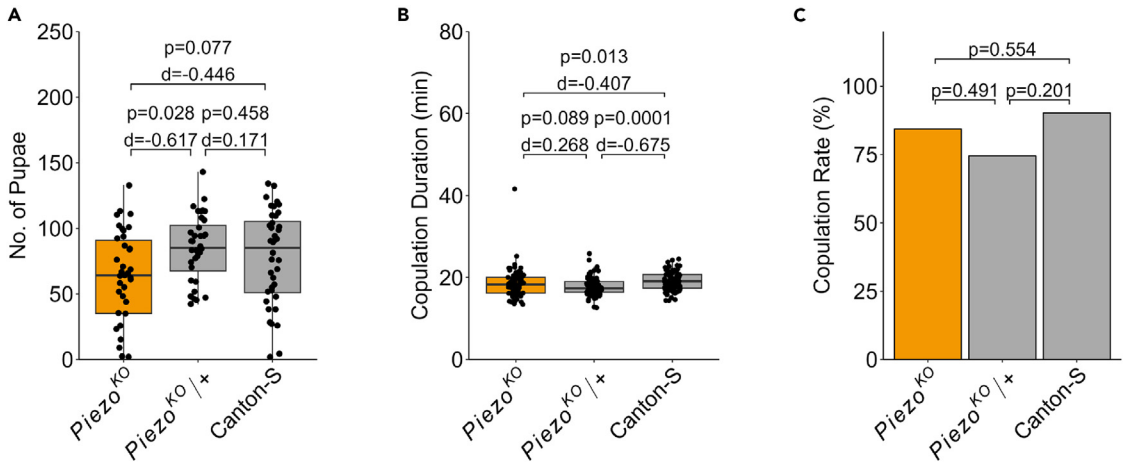

Figure 3. Reduced number of offspring in *Piezo*^{KO} males

(A) The number of pupae produced from a female copulated with a single *Piezo*^{KO}, *Piezo*^{KO}/+, or Canton-S male. ART one-way ANOVA test corrected with the Benjamini-Hochberg method was used for statistical analysis. Boxplots display the medians (horizontal white line in each box) with 25th and 75th percentiles and whiskers denote 1.5x the interquartile range. Each point indicates individual data. p and d indicate the p value and Cohen's d effect size respectively. *Piezo*^{KO}, n = 38; *Piezo*^{KO}/+, n = 36; and Canton-S, n = 40.

(B) Copulation duration for *Piezo*^{KO}, *Piezo*^{KO}/+, and Canton-S males. ART one-way ANOVA test corrected with the Benjamini-Hochberg method was used for statistical analysis. Boxplots display the medians (horizontal white line in each box) with 25th and 75th percentiles and whiskers denote 1.5x the interquartile range. Each point indicates individual data. p and d indicate the p value and Cohen's d effect size respectively. *Piezo*^{KO}, n = 84; *Piezo*^{KO}/+, n = 79; and Canton-S, n = 86.

(C) Copulation success rate for *Piezo*^{KO}, *Piezo*^{KO}/+, and Canton-S males. Fisher's exact test corrected with the Benjamini-Hochberg method was used for statistical analysis. p indicates the p value. *Piezo*^{KO}, n = 51; *Piezo*^{KO}/+, n = 51; and Canton-S, n = 51.

behaviors in copula or by genitalia mis-coupling, and lend support to the hypothesis that *piezo*-mediated mechanosensation in males contributes to stabilizing their copulation postures.

We next tested if unstable copulation posture affected male fertility. Wild-type females that copulated with *Piezo*^{KO} homozygous males produced significantly fewer offspring than those that copulated with heterozygous (*Piezo*^{KO}/+) control males (Figure 3A). At the step of copulation behavior, however, copulation duration and rate for *Piezo*^{KO} homozygous males were virtually identical to those of control males (Figures 3B and 3C). This finding supports the hypothesis that general courtship activity is comparable between *Piezo*^{KO} homozygous males and control males. We further tested for deficits in vitality or physical agility caused by *piezo* mutation. Prior studies reported that Piezo expressed in the digestive organs affects the control of feeding behaviors.[35,36] Accordingly, we observed that locomotor activity and the body size in *Piezo*^{KO} homozygous males were significantly increased compared to control flies (Figures S4A and S4B). These results suggest that general markers of health do not appear compromised in *Piezo*^{KO} homozygous. Moreover, a previous study reported that the body size of males had no significant effect on male fertility,[45] suggesting that the larger body size of *Piezo*^{KO} homozygous males does not cause the reduction of the offspring number.

Fitness reduction in *Piezo*^{KO} homozygous males may be due to lower sperm production. The sizes of the testes, seminal vesicles, and accessory glands, however, appeared similar between *Piezo*^{KO} homozygous males and control males (Figure S4C). Moreover, the seminal vesicles of *Piezo*^{KO} homozygous males contained much sperm, and were indistinguishable from that of control males (Figure S4D). These results suggest that the decreased offspring number of *Piezo*^{KO} homozygous males, who showed unstable copulation postures, is potentially due to inefficient sperm transport rather than spermatogenesis defects.

Stabilizing copulation posture might be important not only in stable conditions but also under disturbances. Under natural conditions, various external stimuli can potentially disturb copulation, such as wind and substrate vibrations.[46–48] We tested if the unstable posture of *Piezo*^{KO} homozygous males affected copulation persistency under physical disturbances by applying mechanical vibrations in the middle of copulation using a vortex mixer. The disturbance was applied 5 min into copulation, when

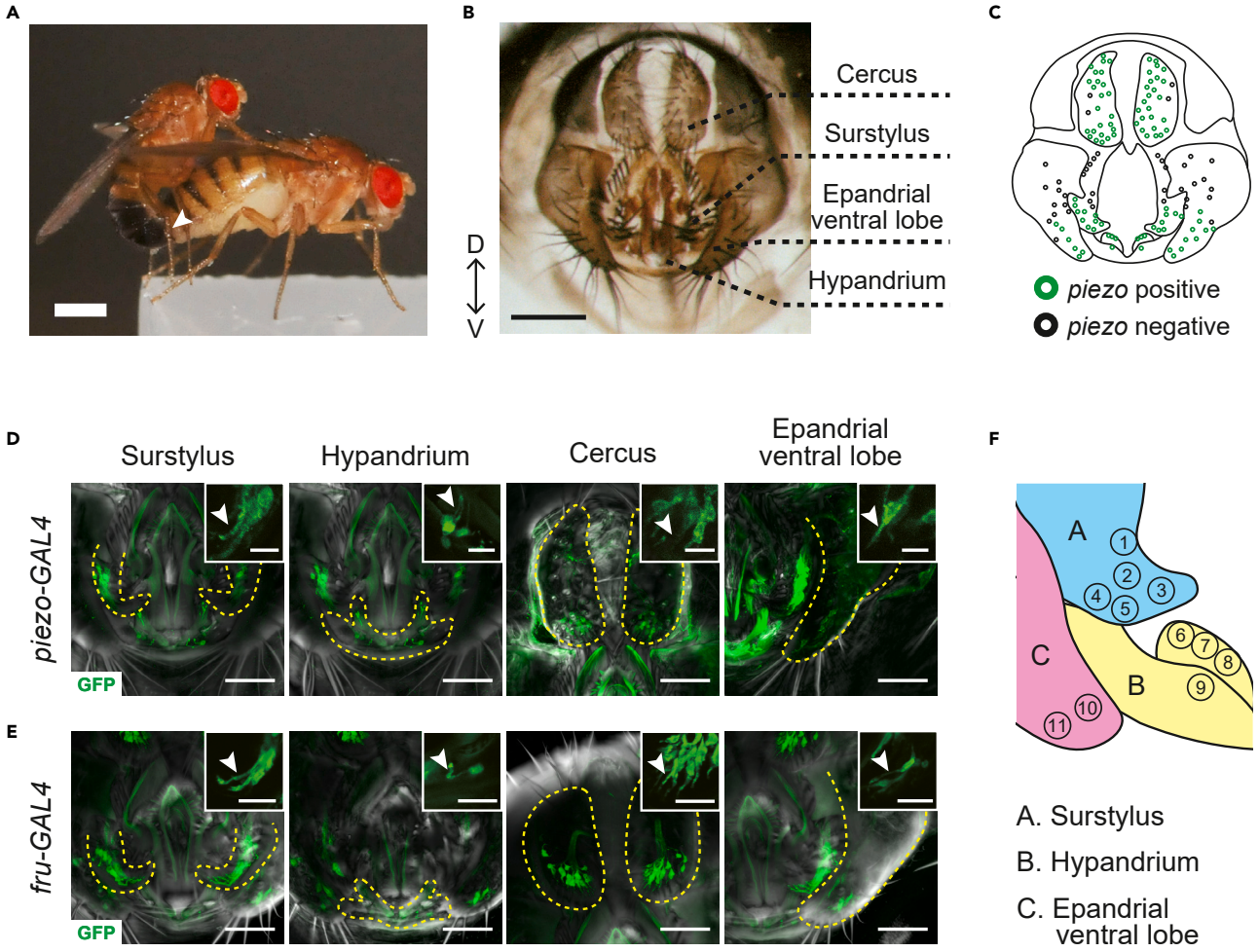

Figure 4. Male genitalia and legs express *piezo*, potentially in the neurons of the mechanosensory bristles

(A) Lateral view of copulating flies. A male interacts with a female through his forelegs and genitalia (white arrowhead). Scale bar, 500 μm.

(B) Male genitalia. D and V indicate the dorsal and ventral sides, respectively. Scale bar, 100 μm.

(C) Schematic of male genitalia. The circles indicate the bristle distributions (green, *piezo* positive; black, *piezo* negative).

(D) *piezo-GAL4* expression in male genital regions. GFP markers driven by *piezo-GAL4* (*piezo-GAL4>20XUAS-IVS-mCD8::GFP*) are detected in surstylus, hypandrium, cercus, and epandrial ventral lobe. The inset in each panel shows a magnified view of the projections to the base of sensory bristles. Yellow dotted lines show each genital region. White arrowheads show each cilium projecting to the bristle. Scale bar, 50 μm (main) or 10 μm (inset).

(E) *fru-GAL4* expression in male genital regions. GFP markers driven by *fru-GAL4* (*fru-GAL4>20XUAS-IVS-mCD8::GFP*) are detected in surstylus, hypandrium, cercus, and epandrial ventral lobe. The inset in each panel shows a magnified view of the projections to the base of sensory bristles. Yellow dotted lines show each genital region. White arrowheads show each cilium projecting to the bristle. Scale bar, 50 μm (main) or 10 μm (inset).

(F) Schematics of surstylus (A, blue), hypandrium (B, yellow), and epandrial ventral lobe (C, pink) in male genitalia. The circled numbers indicate the bristle distributions. The bristle 1 in the surstylus depicts the long mechanosensilla.[21] *piezo-GAL4* positive signals and *fru-GAL4* positive signals were detected in the neurons that project to the base of the no. 1–11 bristles.

"copulation persistence" is at its peak.[48] The ratio of pairs that got separated during the vibrations, however, seemed similar among $Piezo^{KO}$ homozygous males, heterozygous males, and wild-type males (Figure S5). This result suggests that the disruption of *piezo* has less impact on copulation persistency under disturbances, highlighting its role in stabilizing the copulation posture of males under undisturbed conditions.

Inactivation of *piezo* neurons destabilizes copulation

Males interact with females through various body parts, including the genitalia, during copulation (Figure 4A). During copulation, the male genital mechanosensory neurons are suggested to detect genital

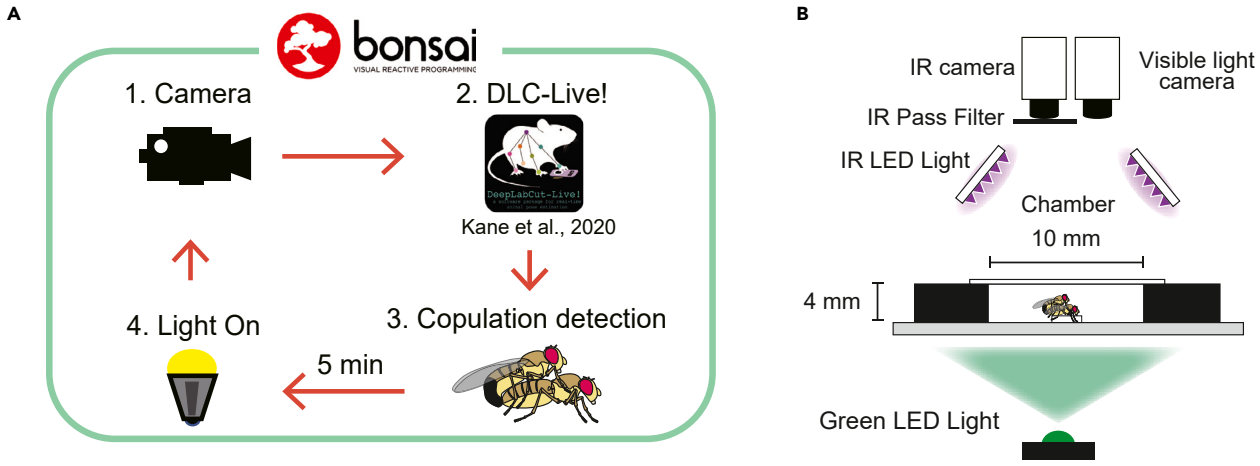
A
bonsai
VISUAL REACTIVE PROGRAMMING
1. Camera
2. DLC-Live!
Kane et al., 2020
3. Copulation detection
4. Light On
5 min

B
IR camera
Visible light camera
IR Pass Filter
IR LED Light
Chamber
10 mm
4 mm
Green LED Light

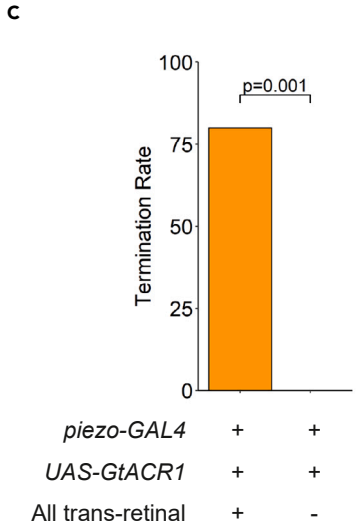
C
p=0.001
Termination Rate
100
75
50
25
0
piezo-GAL4 + +
UAS-GtACR1 + +
All trans-retinal + -

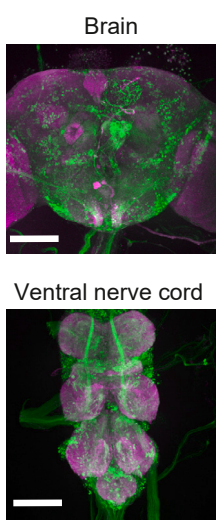
D
Brain
Ventral nerve cord

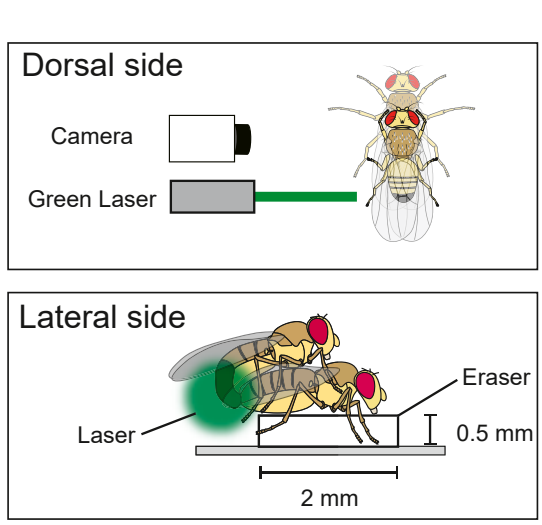
E
Dorsal side
Camera
Green Laser
Lateral side
Laser
Eraser
0.5 mm
2 mm

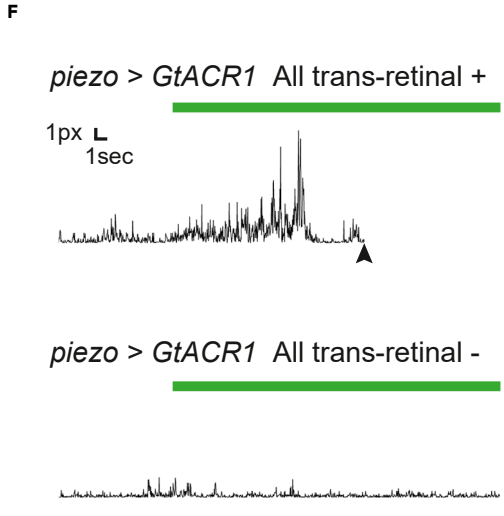
F
piezo > GtACR1 All trans-retinal +
1px
1sec
piezo > GtACR1 All trans-retinal -

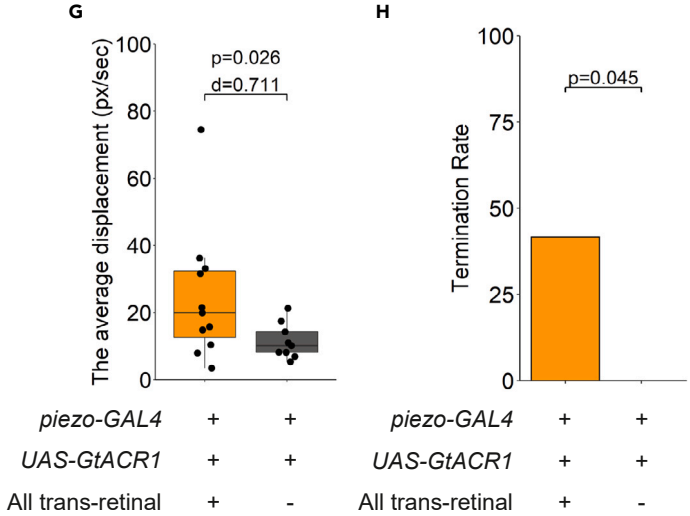
G
The average displacement (px/sec)
p=0.026
d=0.711
100
80
60
40
20
0
piezo-GAL4 + +
UAS-GtACR1 + +
All trans-retinal + -
H
Termination Rate
p=0.045
100
75
50
25
0
piezo-GAL4 + +
UAS-GtACR1 + +
All trans-retinal + -

Figure 5. *piezo*-expressing neurons on the posterior side are involved in copulation maintenance

(A) Schematic of the closed-optogenetic system. This system allows suppression of male *piezo-GAL4* expressing neurons only during copulation. A camera captures the frames (1. Camera), DeepLabCut-Live! (DLC-Live!) detects the body parts (2. DLC-Live!), Bonsai script processes the coordinates of the body parts and detects the copulation event (3. Copulation detection), and the light turns on (4. Light on).

(B) Experimental setup of the optogenetic assays. The infrared (IR) camera and the visible light camera are for observing the flies and time-stamp photostimulations, respectively. The IR light emitting diode (LED) light is used to allow the IR camera to record the flies. The fixed female is placed in the center of the courtship chamber. The green LED is illuminated from the bottom of the chamber for optogenetic inactivation of target neurons.

(C) Rate of copulation termination during optogenetic inactivation of the *piezo-GAL4* expressing neurons in males. Data from experimental (All *trans*-retinal+) and control (All *trans*-retinal−) conditions are shown. Fisher's exact test was used for statistical analysis. p indicates the p value. Experimental, n = 10; and Control, n = 8.

(D) *piezo-GAL4* expression pattern in a representative male brain and ventral nerve cord. Scale bar, 100 μm. Signals of the GFP marker (green) and counter-labeling with the nc82 antibody (magenta) are shown.

(E) Experimental setup for the optogenetic assay with laser. The fixed female is placed in the center of the courtship chamber. Photostimulation with the laser light is applied from one side of the fly. The laser light focuses on the posterior side of the copulating male. The camera is used to confirm the photostimulation region.

(F) Example time traces of male copulation positions. Data for *piezo-GAL4>UAS-GtACR1* males in experimental (Top; All *trans*-retinal+) and control (Bottom; All *trans*-retinal−) conditions are shown. Green horizontal bars indicate the period of the laser photostimulation, which starts 5 min after the copulation initiation. Black arrowhead shows the termination of copulation.

(G) Average displacement of the male copulation position for *piezo-GAL4>UAS-GtACR1* males. The ART one-way ANOVA test was used for statistical analysis. Boxplots display the medians (horizontal white line in each box) with 25th and 75th percentiles and whiskers denote 1.5x the interquartile range. Each point indicates individual data. p and d indicate the p value and Cohen's d effect size respectively. Experimental, n = 12; and Control, n = 9.

(H) Rate of copulation termination during optogenetic inactivation of the *piezo-GAL4* expressing neurons on the posterior side of copulating males. Fisher's exact test was used for statistical analysis. p indicates the p value. Experimental, n = 12; and Control, n = 9.

coupling.[17,23] We, therefore, speculated that unstable copulation in $Piezo^{KO}$ males might be due to the failure of Piezo-mediated mechanosensation in the male genitalia.

It is reported that *piezo* is expressed in sensory neurons and non-neuronal tissues in both adults and larvae.[32] We then evaluated the hypothesis that *piezo*-expressing sensory neurons are involved in the stability of the copulation postures in males. To test if *piezo* is expressed in the sensory neurons of genitalia, we visualized *piezo-GAL4* expressing cells using the *GAL4/UAS* system. In the male genitalia, *piezo-GAL4* positive signals were detected in the mechanosensory neurons that project to the base of sensory bristles in the surstylus (including long and short mechanosensilla[21]), epandrial ventral lobe, cercus, and hypandrum (Figures 4B–4D).

A previous study indicated that *fruitless* (*fru*) -expressing mechanosensory neurons in male genitalia are involved in the copulation duration.[23] We further tested if *fru-GAL4* expression overlapped with *piezo-GAL4* expression in the male genital mechanosensory neurons. *fru-GAL4* positive signals were observed in many mechanosensory neurons of the surstylus, epandrial ventral lobe, cercus, and hypandrum of the male genitalia (Figure 4E), suggesting that many *fru-GAL4* positive signals overlapped with *piezo-GAL4* positive signals in male genital mechanosensory neurons. To evaluate the co-expression of *piezo-GAL4* and *fru-GAL4* signals, we focused on 11 types of bristles on the male genitalia that were identifiable across animals (Figure 4F). For all of these bristles, neurons that projected to the base of each bristle were positive for both *piezo-GAL4* and *fru-GAL4* signals (Figure 4F). To directly confirm the co-expression of *piezo* and *fru*, we combined *piezo-GAL4* and *fru-LexA* and observed overlaps in genitalia by expressing red fluorescent protein (RFP) and GFP markers respectively. This co-expression experiment however yielded only faint signals for both markers (Figures S6A and S6B). Despite these faint signals, we detected an overlap of *piezo-GAL4* positive signals and *fur-LexA* positive signals in a part of mechanosensory neurons that project to the base of sensory bristles in the male genitalia, especially in the surstylus (Figure S6A). Notably, these *piezo-GAL4* and *fru-LexA* double-positive bristles included the long mechanosensilla known to influence male copulation posture.[21] These results strongly suggest that *piezo* and *fru* are expressed in male genitalia, presumably in the mechanosensory neurons of the same sensory bristles.

To investigate the involvement of *piezo*-expressing neurons during copulation, we suppressed these neurons only during copulation. Automated photostimulation systems triggered by selected animal behaviors enable us to conduct optogenetic experiments efficiently with high reproducibility.[49] To this end, we established a DeepLabCut-Live! -based system that recognizes copulation instantly and then automatically controls hardware to silence *piezo*-expressing neurons (Figure 5A). This system tracked body parts of both males and females and detected copulation events based on the distances between them (See Materials

and Methods). In a copulation chamber, we set up a copulation stage to which a wild-type female was attached. A male expressing the green-light-gated anion-channel GtACR1[50] in *piezo*-expressing cells was then introduced to the chamber and video-recorded to allow DeepLabCut-Live! to detect potential copulation events in real-time (Figure 5B). It should be noted that muscle tissue and neuronal cells are potentially affected by GtACR1-mediated suppression.[50] However, expression of the *piezo* gene in the muscle system was not anatomically observed in previous studies,[32] suggesting that only nervous system cells are suppressed in this setup.

Five min after DeepLabCut-Live! had detected the copulation event in each pair, *piezo*-expressing neurons of males were suppressed by green-light photostimulation that covered the entire chamber. During photostimulation, the male's copulation posture was disrupted in the experimental group, in which most pairs terminated copulation, whereas the control pairs were not (Figure 5C, Video S1). This result suggests that the suppression of *piezo*-expressing neurons terminates copulation by disrupting mechanosensation. We also observed that during photostimulation, males typically showed head grooming behaviors with their forelegs while continuing the copulation (Video S1, Figure S7A), possibly due to the suppression of *piezo*-expressing neurons in the head.

The head grooming behaviors observed during photostimulation might be due to the suppression of *piezo*-expressing neurons around the head. In support of this speculation, we confirmed that *piezo-GAL4* positive signals were widely distributed around the head, both in the brain and sensory neurons of Johnston's organ (Figures 5D and S8). A previous study demonstrated that Johnston's organ neurons are responsible for head grooming,[51,52] further supporting the speculation that the head grooming behaviors we observed were due to the manipulation of *piezo*-expressing neurons around the head.

We then narrowed down the *piezo*-expressing neurons responsible for the maintenance of copulation posture by focusing the photostimulation area to gate GtACR1 in *piezo*-expressing neurons using laser illumination which starts 5 min after the copulation initiation. First, we evaluated the illumination area of our experimental setup, using a beam profiler (Figure S9). The intensity distribution data identified a beam diameter of 1.639 mm, which covers about half of a male fly body length (Figure S9B). The laser illumination intensity outside of the laser diameter was too low to induce neuronal inhibition by GtACR1.[50] Using this laser illumination system, we targeted the photostimulation only on the posterior side (focusing on male genitalia) of copulating males to keep the *piezo*-expressing neurons around the head unaffected (Figures 5E and S9A). In the experimental group, this targeted photostimulation destabilized the male's copulation posture significantly after the initiation of photostimulation (Figures 5F and 5G; Video S2) and terminated the copulation (Figure 5H). In contrast, no such tendency was observed in control males (Figures 5F and 5G).

This finding suggests that *piezo*-expressing neurons on the posterior side of the body are responsible for maintaining the copulation posture of males. Interestingly, this targeted photostimulation did not significantly induce head grooming (Video S2, Figure S7B). In contrast, when the male *piezo*-expressing neurons on the anterior side of the body were selectively illuminated, head grooming was observed as observed in the whole body illumination (Video S3, Table S1). In some cases, photostimulation on the anterior side of the male body disrupted copulation in the experimental group (Table S1). These results suggest that the *piezo*-expressing neurons of both the anterior and posterior sides of the body are important for maintaining copulation. In terms of anterior side inhibition, copulation disruption possibly occurred due to *piezo*-expressing neurons in the forelegs and head, the latter of which induces anterior side movements, especially head grooming. In terms of posterior side inhibition, *piezo*-expressing neurons near the genitalia are presumably involved in the maintenance of copulation.

DISCUSSION

Piezo is a mechanosensory channel involved in various *Drosophila* behaviors, such as regulation of feeding behavior and experience-dependent female mating behavior.[32,35,36,38] In addition to this, this study revealed its involvement in male copulation behavior, specifically copulation posture maintenance, for the first time. $Piezo^{KO}$ males tended to tilt during the entire copulation period, indicating the contribution of the Piezo channel in stabilizing copulation posture. We also observed that wild-type females that copulated with $Piezo^{KO}$ males produced significantly fewer offspring. This finding suggests that stabilization of copulation by Piezo is possibly required for increasing offspring number in *Drosophila* males in nature.

Furthermore, inhibiting male *piezo*-expressing neurons on the posterior side of the body during copulation destabilized posture and terminated copulation, lending credence to the idea that these neurons are important for maintaining copulation, or possibly body postures in general.

Previous research in mammals, flies, and nematodes has linked mechanosensation with mating behaviors.[21,23,53,54] In rats, the mechanosensory activity of the penis during mating is suggested to be involved in male ejaculation.[55] In nematodes (*Caenorhabditis elegans*), the MEC-4/MEC-10 mechanoreceptor complex (DeG/ENaC channel) is involved in regulating turning behavior during mating.[56] These findings suggest that mechanosensation is involved in the control of mating behavior, and it is likely conserved across taxa. However, how animals maintain copulation until the gametes are transported to the female reproductive organ remains underexplored. Notable exceptions are found in studies using fruit flies which showed that mechanosensation in male genitalia affected copulation duration and posture,[21,23] suggesting that mechanosensation is involved in copulation maintenance. The male needs to maintain copulation at least until he transfers sufficient sperm for fertile mating, which occurs about 8 min after copulation initiation.[1] We here revealed for the first time the mechanosensory components (i.e., genes and neurons) underlying copulation maintenance of males.

When $Piezo^{KO}$ males were engaged in copulation, the coupling of the male and female genitalia was normal in appearance, but the male copulation posture was unstable and tended to tilt during the entire copulation period (Figure 2). We also demonstrated that the *piezo* mutation in males does not affect the ratio of female kicking behaviors during copulation (Figure S3A). Therefore, female rejection behaviors do not explain the different copulation posture phenotypes observed between $Piezo^{KO}$ and wild-type males. No differences were found in genital touch frequencies prior to copulation initiation either (Figure S3B), suggesting that the *piezo* mutation in males has a particularly pronounced effect during copulation rather than contributing to copulation initiation. Previous studies suggested that some male genital regions (i.e., surstylus, hypandrium, cercus, and epandrial ventral lobe) are involved in grasping the female genitalia during copulation.[15,18,19,57] These regions are covered with sensory bristles that house mechanosensory neurons.[20] Among them, a single pair of long mechanosensilla at the male genital surstylus is known for its importance in the regulation of the copulation posture, as ablation of one of them tends to tilt the copulating males.[21] This phenotype resembles that observed in $Piezo^{KO}$ males. In accordance with this, this study detected the mechanosensory neurons at the sensory bristles of male genital regions as *piezo-GAL4* positive. It can therefore be inferred that the male recognizes the physical coupling with the female genitalia through the male genital *piezo*-expressing mechanosensory neurons and then stabilizes posture during copulation.

Notably, $Piezo^{KO}$ males showed no defects in copulation duration and success rate, whereas inhibition of *piezo*-expressing neurons during copulation induced a severe effect, i.e., copulation termination. A possible reason for this phenotypic difference would be the difference between a gene mutation and neuronal inhibition, as potentially other mechanosensory channels that complement the Piezo function are expressed orthotopically with Piezo. According to the Scope database,[39,40] genes for *piezo* and other mechanosensory channels (i.e., *nompC*, *nan*, and/or *iav*) are co-expressed in the sensory neuron class throughout the body (Figures S10A–S10C). This study finds *nompC-GAL4* positive signals in the mechanosensory neurons that project to the base of sensory bristles in the surstylus of male genitalia, whereas no signal was observed for *nan-GAL4* and *iav-GAL4* (Figures S10D–S10F). This finding suggests that the *nompC* is also responsible for the regulation of copulation posture. Further experiments, which analyze the copulation behavior of males upon disruption of both *piezo* and *nompC*, will shed light on the potentially redundant roles of channel function in the copulation maintenance of male flies.

Our results suggest that mechanosensation mediated by *piezo*-expressing neurons located at the posterior side of the body is necessary to regulate copulation posture in male flies. Moreover, only a few *piezo-GAL4* positive signals were detected at the base of sensory bristles on the male ventral abdomen, which possibly touches the female body during copulation (Figure S11A). It supports the scenario that *piezo*-expressing mechanosensory neurons in male genital regions are part of the neural circuit that regulates the copulation posture of males. On the other hand, inhibition of *piezo*-expressing neurons in the entire body or its anterior side either elicited two major behaviors: copulation termination and head grooming. These observations suggest that terminating copulation primarily involves the *piezo*-expressing neurons on the

posterior side, while head grooming is largely caused by the inhibition of *piezo*-expressing neurons on the anterior side of the fly. A previous study showed that manipulation of a subset of mechanosensory neurons in Johnston's organ (JO neurons), located at the antennae, elicits antennal grooming.[51,52] We found *piezo-GAL4* positive signals in JO neurons (Figure S8), which also supports the possibility that the head grooming behavior we monitored largely depended on manipulation of *piezo*-expressing neurons on the head side. Moreover, *piezo-GAL4* positive signals were also observed at the base of sensory bristles in the forelegs, which hold the female body during copulation (Figure S11B). It is thus likely that *piezo*-expressing neurons in the male forelegs also play a role in maintaining the copulation posture. Our results showed that the frequency of copulation termination via inhibiting *piezo*-expressing neurons was higher during suppression in the entire body than when restricted to the posterior body side. The release of the genital coupling under anterior side illumination is possibly due to the suppression of *piezo*-expressing neurons in the male forelegs and grooming-induced body movement.

A previous study identified a copulation neural circuit of *Drosophila* that mediates the action sequence of copulation from initiation to termination, such as the male genital attachment, intromission, and uncoupling.[17] This copulation neural circuit is comprised mechanosensory neurons, motor neurons, and some interneurons. In this circuit, mechanosensory neurons detect signals from the mechanosensory bristles in the male genitalia. A retrograde labeling experiment showed that they send their axons to the male abdominal ganglion and synapse to motor neurons,[17] possibly transmitting the sensory information directly to the motor neurons there from the genitalia. The motor neurons in this circuit, in turn, regulate the phallic and periphallic musculature in the male genitalia, by which adjusts the genital grasping of the female genitalia[22] depending on the mechanosensory inputs.[17] A part of the mechanosensory neurons in this circuit was suggested to express *fru* gene.[23] This previous research suggests that the *fru*-expressing sensory neurons in this circuit send signals to the motor neurons to adjust the appropriate positioning of the male throughout an entire copulation event by controlling the male genital grasping of the female genitalia.

In this study, we found that cell bodies of *piezo-GAL4* positive mechanosensory neurons innervating the genitalia are located in the abdominal ganglion and their peripheral ends projected to the genital mechanosensory bristles. These *piezo-GAL4* positive sensory neurons mostly overlapped with the distribution of *fru*-positive sensory neurons in male genitalia (Figures 4D–4F and S6). Previous studies reported that the mechanosensory neurons in the copulation neural circuit express *fru*, but which mechanosensory genes were expressed in these neurons remained unclear.[17,23] Our results suggest that *piezo* is expressed in the mechanosensory neurons of the copulation circuit for transmitting signals from the genital mechanosensory bristles (Figures 4B–4E).[17,23] In addition, the mechanosensory neurons that projected to the male genital long mechanosensilla, whose ablation induced the tilted copulation postures in wild-type males,[21] were positive for both *piezo-GAL4* and *fru-GAL4* signals (Figure S6). Our findings together suggest that the *piezo-GAL4* positive neurons in the male genitalia possibly receive mechanosensory input during copulation and then transmit signals to the copulation neural circuit that adjusts the phallic and periphallic musculature, resulting in copulation maintenance.

Piezo^{KO} males showed reduced fertility, indicating reduced fitness. Unexpectedly, we found that *Piezo*^{KO} males have no obvious defect in copulation duration and copulation rate. We also showed that the reduction of male fertility resulting from *piezo* mutation was unlikely to be caused by general deficits in the fly's health or decreased sperm levels in male reproductive organs. The reduced male fertility found in *Piezo*^{KO} males is, therefore, possibly caused by reductions in sperm transport due to disrupted copulation posture. It is also possible that *Piezo*^{KO} males fail to detect mechanosensory input during copulation, resulting in a lower amount of sperm being transported. Further research is needed to investigate these possibilities, e.g., by determining if the *Piezo*^{KO} males reduce the amount of sperm delivered to the female's internal reproductive organs. Furthermore, since we have not directly evaluated the fertilizing ability of *Piezo*^{KO} male sperm, the reduced fertility observed in these males may also be attributable to impaired sperm function.

In *Drosophila*, copulating males adjust the number of their sperm transferred based on the female mating status, fecundity, and age.[58] It has been suggested that the male senses the female's state and regulates the number of sperm to transfer, possibly by detecting pheromones from the female.[58] The findings of this study propose another type of signal with which the male detects the female's condition in copula, i.e., the

mechanosensory signal mediated via *piezo*-expressing mechanosensory neurons, to regulate the number of their sperm. The transfer of sperm and seminal fluid depends on the activation of neurons in the abdominal ganglion that co-express *fru* and *corazonin* (*crz*).[1] The mechanism that regulates the activity of fru^+crz^+ neurons remains unclear. An interesting possibility is that fru^+crz^+ neuronal activity is controlled by the mechanical senses via *piezo*-expressing neurons. To evaluate this possibility, the functional connection between sperm transport and mechanosensation is to be confirmed by observing the activity of fru^+crz^+ neurons in the abdominal ganglion during mechanical stimulation from the genitalia (or optogenetic activation of *piezo*-expressing neurons) using calcium imaging.

This study shows for the first time that Piezo and *piezo*-expressing neurons are necessary for stabilizing copulation posture and maintenance, respectively, in male *D. melanogaster*. Although it remains to be tested whether reduced fertility in $Piezo^{KO}$ males could be rescued by forced expression of *piezo*, our findings suggest that copulation maintenance and stabilization of copulation by Piezo is possibly required for increasing offspring number for male flies. In adult *D. melanogaster* females, *piezo* is expressed in reproductive organs, and mechanosensation mediated by Piezo channels contributes to the female mating experience.[38] Piezo-mediated mechanosensation via genitalia would be, therefore, important for both males and females. The *piezo* homologs are widely found among various species[59] and homologous genes of *piezo* exist even in plants and protists,[59] implying that Piezo channels regulate many physiological processes across organisms. Additionally, Piezo has been implicated in underpinning the mating behaviors of males. In mammals, two types of Piezo channels (Piezo1 and Piezo2) are responsible for detecting mechanical stimuli and converting them into electrical signals.[59] In mice, Piezo1, a homolog of the *piezo* family, was found in some structures of male internal genitalia (i.e., prostate gland, seminal vesicles, and ejaculatory ducts), suggesting that Piezo1 serves a role in detecting the amounts of glandular content and possibly involved in the contraction and release of glandular secretions during ejaculation.[42] In a wild-type rat subpopulation that shows premature ejaculation, the knockdown of *Piezo2*, another homolog in the *piezo* family, significantly improved the ejaculation latency, as well as mounting frequency and ejaculation frequency.[55] This research implies the involvement of Piezo channels in male ejaculation and mounting in mammals. In *C. elegans*, mechanosensation is involved in the control of the mating behavior.[54] *pezo-1*, a *C. elegans* homolog in the *piezo* family, is expressed in male-specific neurons with key roles in mating behavior; *pezo-1* mutations compromise mating efficiency and multiple steps of mating behaviors in *C. elegans* males.[60] These findings in mice, rats, and *C. elegans* together suggest that the mechanism to control mating behaviors through Piezo-mediated mechanosensation is widely shared across animal species that engage in mating behavior. Although prior studies have suggested the involvement of Piezo-mediated mechanosensation during mating, there has been little research on the mechanosensation underlying copulation maintenance. This study reveals for the first time that the mechanosensory system, mediated via Piezo channels, contributes to copulation maintenance and male fitness and opens a new avenue for revealing the copulation maintenance mechanism through mechanosensation.

Limitations of the study

Our study demonstrated that a mechanosensory gene *piezo* and its expressing neurons are responsible for copulation maintenance in *Drosophila* males. Our findings suggest that copulation maintenance mediated by Piezo possibly increases the fitness of males by stabilizing copulation. We attempted to limit the photostimulation area used to gate the GtACR1 in *piezo*-expressing neurons using a laser. Although we narrowed down the responsible neurons to those located in the posterior side of the male body, a lack of appropriate genetic tools prevented us from directly evaluating if *piezo*-expressing neurons in the sensory bristles on the male genitalia mediate copulation maintenance. This is due to the difficulty of labeling and manipulating specific peripheral *piezo*-expressing neurons. Previous research suggests that the male genital mechanosensory neurons are connected to the motor neurons that innervate male genital muscles and are involved in the copulation maintenance.[17,23] Building on these previous studies, we hypothesize that *piezo*-expressing mechanosensory neurons that send their cilia to sensory bristles on the male genitalia detect the genital coupling, and by doing so contribute to copulation maintenance.

We showed $Piezo^{KO}$ males produced significantly fewer offspring than control males. This phenotype is unlikely to be due to general effects such as reduced locomotor activity or nutritional deficits resulting from *piezo* mutation. We hypothesize that reduced fertility was due to $Piezo^{KO}$ males delivering less sperm to

females than wild-type males. Due to technical limitations, however, we were not able to directly evaluate this idea by counting sperm in female reproductive organs.

STAR★METHODS

Detailed methods are provided in the online version of this paper and include the following:

- KEY RESOURCES TABLE
- RESOURCE AVAILABILITY
  - Lead contact
  - Materials availability
  - Data and code availability
- EXPERIMENTAL MODEL AND SUBJECT DETAILS
  - Fly strain
- METHOD DETAILS
  - Dissection and immunolabeling
  - Confocal microscopy and image processing
  - Video recordings
  - Copulation assays
  - Copulation disturbance assays
  - Creation of the DeepLabCut models
  - Evaluation of male copulation posture
  - Optogenetic assays – retinal feeding
  - Optogenetic assays - fixing females
  - Optogenetic assays - photostimulation
  - Optogenetic assays – laser profiling
  - Optogenetic assays - A closed-loop system
  - Manual behavior analysis
  - Locomotor activity analysis
- QUANTIFICATION AND STATISTICAL ANALYSIS

SUPPLEMENTAL INFORMATION

Supplemental information can be found online at https://doi.org/10.1016/j.isci.2023.106617.

ACKNOWLEDGMENTS

We thank Dr. Yoichi Oda, Dr. Yuki Ishikawa, Dr. Matthew P. Su, and Dr. Daniel F. Eberl for discussions; Dr. Ryosuke F. Takeuchi for Bonsai scripts; Mr. Ryota Nishimura for production of the chambers used in behavioral experiments; Dr. Shin Sugiyama for technical assistance of the dissection of internal reproductive organs; Mr. Yuichiro Ito for technical assistance of locomotor activity assay; Dr. Kosuke Murate and Dr. Akiyoshi Hishikawa for laser profiling; Dr. Kei Ito, Dr. Barry Dickson, Dr. Bruce S. Baker, Vienna *Drosophila* Resource Center, and Bloomington *Drosophila* Stock Center for fly stocks; Developmental Studies Hybridoma Bank for antibodies. This study was supported by MEXT KAKENHI Grants-in-Aid for Scientific Research (B) (grant JP20H03355 to AK), Scientific Research on Innovative Areas "Evolinguistics" (grant JP20H04997 to AK), Grant-in-Aid for Transformative Research Areas (A) "iPlasticity" (grant JP21H05689 to A.K.), Grant-in Aid for Early-Career Scientists (grants JP19K16186 and JP21K15137 to R.T.), Grant-in Aid for Transformative Research Areas (A) Hierarchical Bio-Navigation (grant JP22H05650 to R.T.) and JST FOREST (grant JPMJFR2147 to AK), Japan.

AUTHOR CONTRIBUTIONS

H. M. Y.: Conceptualization, Methodology, Software, Validation, Formal analysis, Investigation, Data curation, Visualization, Writing – original draft; R. T.: Conceptualization, Methodology, Validation, Investigation, Supervision, Project Administration, Funding Acquisition, Writing – original draft; A. K.: Validation, Investigation, Supervision, Project Administration, Funding Acquisition, Writing – original draft.

DECLARATION OF INTERESTS

The authors declare no competing interests.

INCLUSION AND DIVERSITY

We support inclusive, diverse, and equitable conduct of research.

Received: December 12, 2022
Revised: March 13, 2023
Accepted: April 4, 2023
Published: April 11, 2023

REFERENCES

1. Tayler, T.D., Pacheco, D.A., Hergarden, A.C., Murthy, M., and Anderson, D.J. (2012). A neuropeptide circuit that coordinates sperm transfer and copulation duration in *Drosophila*. Proc. Natl. Acad. Sci. USA *109*, 20697–20702. https://doi.org/10.1073/pnas.1218246109.

2. Latham, K.L., Liu, Y.S., and Taylor, B.J. (2013). A small cohort of FRUM and Engrailed-expressing neurons mediate successful copulation in *Drosophila melanogaster*. BMC Neurosci. *14*, 57. https://doi.org/10.1186/1471-2202-14-57.

3. Huber, B.A., Sinclair, B.J., and Schmitt, M. (2007). The evolution of asymmetric genitalia in spiders and insects. Biol. Rev. *82*, 647–698. https://doi.org/10.1111/j.1469-185X.2007.00029.x.

4. Inatomi, M., Shin, D., Lai, Y.T., and Matsuno, K. (2019). Proper direction of male genitalia is prerequisite for copulation in *Drosophila*, implying cooperative evolution between genitalia rotation and mating behavior. Sci. Rep. *9*, 210–212. https://doi.org/10.1038/s41598-018-36301-7.

5. Arnqvist, G., and Rowe, L. (2002). Antagonistic coevolution between the sexes in a group of insects. Nature *415*, 787–789. https://doi.org/10.1038/415787a.

6. Arnqvist, G., and Rowe, L. (2002). Correlated evolution of male and female morphologies in water striders. Evolution *56*, 936–947. https://doi.org/10.1111/j.0014-3820.2002.tb01406.x.

7. Greenspan, R.J., and Ferveur, J.F. (2000). Courtship in *Drosophila*. Annu. Rev. Genet. *34*, 205–232. https://doi.org/10.1146/annurev.genet.34.1.205.

8. Riemensperger, T., Kittel, R.J., and Fiala, A. (2016). Optogenetics in *Drosophila* neuroscience. Methods Mol. Biol. *1408*, 167–175. https://doi.org/10.1007/978-1-4939-3512-3_11.

9. Tolwinski, N.S. (2017). Introduction: *Drosophila*-A model system for developmental biology. J. Dev. Biol. *5*, 9–11. https://doi.org/10.3390/jdb5030009.

10. Villella, A., and Hall, J.C. (2008). Chapter 3 Neurogenetics of courtship and mating in *Drosophila*. Adv. Genet. *62*, 67–184. https://doi.org/10.1016/S0065-2660(08)00603-2.

11. Ishimoto, H., and Kamikouchi, A. (2021). Molecular and neural mechanisms regulating sexual motivation of virgin female *Drosophila*. Cell. Mol. Life Sci. *78*, 4805–4819. https://doi.org/10.1007/s00018-021-03820-y.

12. Sturtevant, A.H. (1915). Experiments on sex recognition and the problem of sexual selection in Drosoophilia. J. Anim. Behav. *5*, 351–366. https://doi.org/10.1037/h0074109.

13. Billeter, J.C., Rideout, E.J., Dornan, A.J., and Goodwin, S.F. (2006). Control of male sexual behavior in *Drosophila* by the sex determination pathway. Curr. Biol. *16*, R766–R776. https://doi.org/10.1016/j.cub.2006.08.025.

14. Fowler, G.L. (1973). Some aspects of the reproductive biology of *Drosophila*: sperm transfer, sperm storage, and sperm utilization. Adv. Genet. *17*, 293–360. https://doi.org/10.1016/S0065-2660(08)60173-X.

15. Jagadeeshan, S., and Singh, R.S. (2006). A time-sequence functional analysis of mating behaviour and genital coupling in *Drosophila*: role of cryptic female choice and male sex-drive in the evolution of male genitalia. J. Evol. Biol. *19*, 1058–1070. https://doi.org/10.1111/j.1420-9101.2006.01099.x.

16. Massey, J.H., Chung, D., Siwanowicz, I., Stern, D.L., and Wittkopp, P.J. (2019). The *yellow* gene influences *Drosophila* male mating success through sex comb melanization. Elife *8*, 493888–e49420. https://doi.org/10.7554/eLife.49388.

17. Pavlou, H.J., Lin, A.C., Neville, M.C., Nojima, T., Diao, F., Chen, B.E., White, B.H., and Goodwin, S.F. (2016). Neural circuitry coordinating male copulation. Elife *5*, e20713. https://doi.org/10.7554/eLife.20713.001.

18. Mattei, A.L., Riccio, M.L., Avila, F.W., Wolfner, M.F., and Denlinger, D.L. (2015). Integrated 3D view of postmating responses by the *Drosophila melanogaster* female reproductive tract, obtained by micro-computed tomography scanning. Proc. Natl. Acad. Sci. USA *112*, 8475–8480. https://doi.org/10.1073/pnas.1505797112.

19. Kamimura, Y., and Mitsumoto, H. (2011). Comparative copulation anatomy of the *Drosophila melanogaster* species complex (Diptera: drosophilidae). Entomol. Sci. *14*, 399–410. https://doi.org/10.1111/j.1479-8298.2011.00467.x.

20. Taylor, B.J. (1989). Sexually dimorphic neurons of the terminalia of Sex-specific axonal arborizations in the central nervous system. J. Neurogenet. *5*, 193–213. https://doi.org/10.3109/01677068909066208.

21. Acebes, A., Cobb, M., and Ferveur, J.F. (2003). Species-specific effects of single sensillum ablation on mating position in *Drosophila*. J. Exp. Biol. *206*, 3095–3100. https://doi.org/10.1242/jeb.00522.

22. Kamimura, Y. (2010). Copulation anatomy of *Drosophila melanogaster* (Diptera: drosophilidae): wound-making organs and their possible roles. Zoomorphology *129*, 163–174. https://doi.org/10.1007/s00435-010-0109-5.

23. Jois, S., Chan, Y.-B., Fernandez, M.P., Pujari, N., Janz, L.J., Parker, S., and Leung, A.K.-W. (2022). Sexually dimorphic peripheral sensory neurons regulate copulation duration and persistence in male *Drosophila*. Sci. Rep. *12*, 6177–6212. https://doi.org/10.1038/s41598-022-10247-3.

24. Hehlert, P., Zhang, W., and Göpfert, M.C. (2021). *Drosophila* mechanosensory transduction. Trends Neurosci. *44*, 323–335. https://doi.org/10.1016/j.tins.2020.11.001.

25. Eberl, D.F., Hardy, R.W., and Kernan, M.J. (2000). Genetically similar transduction mechanisms for touch and hearing in *Drosophila*. J. Neurosci. *20*, 5981–5988. https://doi.org/10.1523/jneurosci.20-16-05981.2000.

26. Kim, J., Chung, Y.D., Park, D.Y., Choi, S., Shin, D.W., Soh, H., Lee, H.W., Son, W., Yim, J., Park, C.S., et al. (2003). A TRPV family ion channel required for hearing in *Drosophila*. Nature *424*, 81–84. https://doi.org/10.1038/nature01733.

27. Gong, Z., Son, W., Chung, Y.D., Kim, J., Shin, D.W., McClung, C.A., Lee, Y., Lee, H.W., Chang, D.J., Kaang, B.K., et al. (2004). Two interdependent TRPV channel subunits, inactive and nanchung, mediate hearing in *Drosophila*. J. Neurosci. *24*, 9059–9066. https://doi.org/10.1523/JNEUROSCI.1645-04.2004.

28. Nesterov, A., Spalthoff, C., Kandasamy, R., Katana, R., Rankl, N.B., Andrés, M., Jähde, P., Dorsch, J.A., Stam, L.F., Braun, F.J., et al. (2015). TRP channels in insect stretch receptors as insecticide targets. Neuron *86*, 665–671. https://doi.org/10.1016/j.neuron.2015.04.001.

29. Effertz, T., Wiek, R., and Göpfert, M.C. (2011). NompC TRP channel is essential for *Drosophila* sound receptor function. Curr. Biol. *21*, 592–597. https://doi.org/10.1016/j.cub.2011.02.048.

30. Kernan, M., Cowan, D., and Zuker, C. (1994). Genetic dissection of mechanosensory

transduction : mechanoreception-defective mutations of *Drosophila*. Neuron *12*, 1195–1206. https://doi.org/10.1016/0896-6273(94)90437-5.

31. Yan, Z., Zhang, W., He, Y., Gorczyca, D., Xiang, Y., Cheng, L.E., Meltzer, S., Jan, L.Y., and Jan, Y.N. (2013). *Drosophila* NOMPC is a mechanotransduction channel subunit for gentle-touch sensation. Nature *493*, 221–225. https://doi.org/10.1038/nature11685.

32. Kim, S.E., Coste, B., Chadha, A., Cook, B., and Patapoutian, A. (2012). The role of *Drosophila* Piezo in mechanical nociception. Nature *483*, 209–212. https://doi.org/10.1038/nature10801.

33. Murthy, S.E., Dubin, A.E., and Patapoutian, A. (2017). Piezos thrive under pressure: mechanically activated ion channels in health and disease. Nat. Rev. Mol. Cell Biol. *18*, 771–783. https://doi.org/10.1038/nrm.2017.92.

34. Moroni, M., Servin-Vences, M.R., Fleischer, R., Sánchez-Carranza, O., and Lewin, G.R. (2018). Voltage gating of mechanosensitive PIEZO channels. Nat. Commun. *9*, 1096–1115. https://doi.org/10.1038/s41467-018-03502-7.

35. Wang, P., Jia, Y., Liu, T., Jan, Y.N., and Zhang, W. (2020). Visceral mechano-sensing neurons control *Drosophila* feeding by using Piezo as a sensor. Neuron *108*, 640–650.e4. https://doi.org/10.1016/j.neuron.2020.08.017.

36. Min, S., Oh, Y., Verma, P., Whitehead, S.C., Yapici, N., Van Vactor, D., Suh, G.S., and Liberles, S. (2021). Control of feeding by Piezo-mediated gut mechanosensation in *Drosophila*. Elife *10*, e63049–e63218. https://doi.org/10.7554/eLife.63049.

37. Oh, Y., Lai, J.S.Y., Min, S., Huang, H.W., Liberles, S.D., Ryoo, H.D., and Suh, G.S.B. (2021). Periphery signals generated by Piezo-mediated stomach stretch and Neuromedin-mediated glucose load regulate the *Drosophila* brain nutrient sensor. Neuron *109*, 1979–1995.e6. https://doi.org/10.1016/j.neuron.2021.04.028.

38. Shao, L., Chung, P., Wong, A., Siwanowicz, I., Kent, C.F., Long, X., and Heberlein, U. (2019). A neural circuit encoding the experience of copulation in female *Drosophila*. Neuron *102*, 1025–1036.e6. https://doi.org/10.1016/j.neuron.2019.04.009.

39. Li, H., Janssens, J., Waegeneer, M.D., Kolluru, S.S., Davie, K., Spanier, K., Leskovec, J., Mclaughlin, C.N., Xie, Q., Jones, R.C., et al. (2022). Fly Cell Atlas: a single-nucleus transcriptomic atlas of the adult fruit fly. Science *2432*. https://doi.org/10.1126/science.abk2432.

40. Davie, K., Janssens, J., Koldere, D., De Waegeneer, M., Pech, U., Kreft, Ł., Aibar, S., Makhzami, S., Christiaens, V., Bravo González-Blas, C., et al. (2018). A single-cell transcriptome atlas of the aging *Drosophila* brain. Cell *174*, 982–998.e20. https://doi.org/10.1016/j.cell.2018.05.057.

41. DiAntonio, A., Burgess, R.W., Chin, A.C., Deitcher, D.L., Scheller, R.H., and Schwarz, T.L. (1993). Identification and characterization of *Drosophila* genes for synaptic vesicle proteins. J. Neurosci. *13*, 4924–4935. https://doi.org/10.1523/jneurosci.13-11-04924.1993.

42. Dalghi, M.G., Clayton, D.R., Ruiz, W.G., Al-bataineh, M.M., Satlin, L.M., Kleyman, T.R., Ricke, W.A., Carattino, M.D., and Apodaca, G. (2019). Expression and distribution of PIEZO1 in the mouse urinary tract. Am. J. Physiol. Ren. Physiol. *317*, 303–321. https://doi.org/10.1152/ajprenal.00214.2019.

43. Mathis, A., Mamidanna, P., Cury, K.M., Abe, T., Murthy, V.N., Mathis, M.W., and Bethge, M. (2018). DeepLabCut: markerless pose estimation of user-defined body parts with deep learning. Nat. Neurosci. *21*, 1281–1289. https://doi.org/10.1038/s41593-018-0209-y.

44. Acurio, A.E., Rhebergen, F.T., Paulus, S., Courtier-Orgogozo, V., and Lang, M. (2019). Repeated evolution of asymmetric genitalia and right-sided mating behavior in the *Drosophila nannoptera* species group. BMC Evol. Biol. *19*, 109–114. https://doi.org/10.1186/s12862-019-1434-z.

45. Lefranc, A., and Bundgaard, J. (2000). The influence of male and female body size on copulation duration and fecundity in *Drosophila melanogaster*. Hereditas (Lund) *132*, 243–247. https://doi.org/10.1111/j.1601-5223.2000.00243.x.

46. Foster, S.P., and Harris, M.O. (1997). Behavioral manipulation methods for insect pest-management. Annu. Rev. Entomol. *42*, 123–146. https://doi.org/10.1146/annurev.ento.42.1.123.

47. Polajnar, J., Eriksson, A., Lucchi, A., Anfora, G., Virant-Doberlet, M., and Mazzoni, V. (2015). Manipulating behaviour with substrate-borne vibrations - potential for insect pest control. Pest Manag. Sci. *71*, 15–23. https://doi.org/10.1002/ps.3848.

48. Crickmore, M.A., and Vosshall, L.B. (2013). Opposing dopaminergic and GABAergic neurons control the duration and persistence of copulation in *Drosophila*. Cell *155*, 881–893. https://doi.org/10.1016/j.cell.2013.09.055.

49. Yamanouchi, H.M., Tanaka, R., and Kamikouchi, A. (2023). Event-triggered feedback system using YOLO for optogenetic manipulation of neural activity. IEEE Int. Conf. Pervasive Comput. Commun. Work. Other Affil. Events (PerCom Work. BiRD 2023) (In press).

50. Mohammad, F., Stewart, J.C., Ott, S., Chlebikova, K., Chua, J.Y., Koh, T.W., Ho, J., and Claridge-Chang, A. (2017). Optogenetic inhibition of behavior with anion channelrhodopsins. Nat. Methods *14*, 271–274. https://doi.org/10.1038/nmeth.4148.

51. Hampel, S., Eichler, K., Yamada, D., Bock, D.D., Kamikouchi, A., and Seeds, A.M. (2020). Distinct subpopulations of mechanosensory chordotonal organ neurons elicit grooming of the fruit fly antennae. Elife *9*, 599766–e60026. https://doi.org/10.7554/eLife.59976.

52. Hampel, S., Franconville, R., Simpson, J.H., and Seeds, A.M. (2015). A neural command circuit for grooming movement control. Elife *4*, 087588–e8826. https://doi.org/10.7554/eLife.08758.

53. Soni, K.K., Jeong, H.S., and Jang, S. (2022). Neurons for ejaculation and factors affecting ejaculation. Biology *11*, 686. https://doi.org/10.3390/biology11050686.

54. Barr, M.M., and Garcia, L.R. (2006). Male mating behavior. Worm *1–11*. https://doi.org/10.1895/wormbook.1.78.1.

55. Chen, Z., Yuan, M., Ma, Z., Wen, J., Wang, X., Zhao, M., Liu, J., Zhang, X., Zhao, S., and Guo, L. (2020). Significance of piezo-type mechanosensitive ion channel component 2 in premature ejaculation: an animal study. Andrology *8*, 1347–1359. https://doi.org/10.1111/andr.12779.

56. Liu, T., Kim, K., Li, C., and Barr, M.M. (2007). FMRFamide-like neuropeptides and mechanosensory touch receptor neurons regulate male sexual turning behavior in *Caenorhabditis elegans*. J. Neurosci. *27*, 7174–7182. https://doi.org/10.1523/JNEUROSCI.1405-07.2007.

57. Frazee, S.R., and Masly, J.P. (2015). Multiple sexual selection pressures drive the rapid evolution of complex morphology in a male secondary genital structure. Ecol. Evol. *5*, 4437–4450. https://doi.org/10.1002/ece3.1721.

58. Lüpold, S., Manier, M.K., Ala-Honkola, O., Belote, J.M., and Pitnick, S. (2011). Male *Drosophila melanogaster* adjust ejaculate size based on female mating status, fecundity, and age. Behav. Ecol. *22*, 184–191. https://doi.org/10.1093/beheco/arq193.

59. Coste, B., Mathur, J., Schmidt, M., Earley, T.J., Ranade, S., Petrus, M.J., Dubin, A.E., and Patapoutian, A. (2010). Piezo1 and Piezo2 are essential components of distinct mechanically activated cation channels. Science *330*, 55–60. https://doi.org/10.1126/science.1193270.

60. Brugman, K.I., Susoy, V., Whittaker, A.J., Palma, W., Nava, S., Samuel, A.D.T., and Sternberg, P.W. (2022). PEZO-1 and TRP-4 mechanosensors are involved in mating behavior in *Caenorhabditis elegans*. PNAS Nexus *1*. pgac213-26. https://doi.org/10.1093/pnasnexus/pgac213.

61. Pfeiffer, B.D., Ngo, T.T.B., Hibbard, K.L., Murphy, C., Jenett, A., Truman, J.W., and Rubin, G.M. (2010). Refinement of tools for targeted gene expression in *Drosophila*. Genetics *186*, 735–755. https://doi.org/10.1534/genetics.110.119917.

62. Yamada, D., Ishimoto, H., Li, X., Kohashi, T., Ishikawa, Y., and Kamikouchi, A. (2018). GABAergic local interneurons shape female fruit fly response to mating songs. J. Neurosci. *38*, 4329–4347.

https://doi.org/10.1523/JNEUROSCI.3644-17.2018.

63. Manning, A. (1967). The control of sexual receptivity in female *Drosophila*. Anim. Behav. *15*, 239–250. https://doi.org/10.1016/0003-3472(67)90006-1.

64. Rhebergen, F.T., Courtier-Orgogozo, V., Dumont, J., Schilthuizen, M., and Lang, M. (2016). *Drosophila pachea* asymmetric lobes are part of a grasping device and stabilize one-sided mating. BMC Evol. Biol. *16*, 176. https://doi.org/10.1186/s12862-016-0747-4.

65. Lopes, G., Bonacchi, N., Frazão, J., Neto, J.P., Atallah, B.V., Soares, S., Moreira, L., Matias, S., Itskov, P.M., Correia, P.A., et al. (2015). Bonsai: an event-based framework for processing and controlling data streams. Front. Neuroinf. *9*, 1–14. https://doi.org/10.3389/fninf.2015.00007.

66. Kane, G.A., Lopes, G., Saunders, J.L., Mathis, A., and Mathis, M.W. (2020). Real-time, low-latency closed-loop feedback using markerless posture tracking. Elife *9*, e61909–e61929. https://doi.org/10.7554/ELIFE.61909.

67. Wobbrock, J.O., Findlater, L., Gergle, D., and Higgins, J.J. (2011). The aligned rank transform for nonparametric factorial analyses using only ANOVA procedures. In Proceedings of the ACM Conference on Human Factors in Computing Systems (CHI 2011). https://doi.org/10.1145/1978942.1978963.

68. Kay, M., Elkin, L.A., Higgins, J.J., and Wobbrock, J.O. (2021). ARTool: Aligned Rank Transform for Nonparametric Factorial Anovas, p. 594511. R package version 0.11.1. https://doi.org/10.5281/zenodo.594511. https://github.com/mjskay/ARTool.

STAR★METHODS

KEY RESOURCES TABLE

REAGENT or RESOURCE	SOURCE	IDENTIFIER
Antibodies		
Rabbit anti-GFP	Invitrogen	Cat# A11122; RRID: AB_221569
Mouse nc82 (supernatant)	Developmental Studies Hybridoma Bank	Cat# nc82; RRID:AB_2314866
Alexa Fluor 488 anti-Rabbit	Invitrogen	Cat# A11034; RRID:AB_2576217
Alexa Fluor 647 anti-Mouse	Invitrogen	Cat# A21236; RRID: AB_2535805
Chemicals, peptides, and recombinant proteins		
DAPI	Sigma-Aldrich	Cat# D9542
all trans-retinal	Sigma-Aldrich	Cat# R2500
Experimental models: Organisms/strains		
D. melanogaster: Canton-S	Hotta-lab strain, a gift from Dr. Kei Ito	N/A
D. melanogaster: piezo^{KO}	Bloomington *Drosophila* Stock Center	BDSC: 58770; RRID: BDSC_58770
D. melanogaster: w^{1118}	Vienna *Drosophila* Resource Center	VDRC: 60000
D. melanogaster: piezo-GAL4 (Chr 3)	Bloomington *Drosophila* Stock Center	BDSC: 59266; RRID: BDSC_59266
D. melanogaster: piezo-GAL4 (Chr 2)	Bloomington *Drosophila* Stock Center	BDSC: 58771; RRID: BDSC_58711
D. melanogaster: iav-GAL4	Bloomington *Drosophila* Stock Center	BDSC: 52273; RRID: BDSC_52273
D. melanogaster: nan-GAL4	Bloomington *Drosophila* Stock Center	BDSC: 24903; RRID: BDSC_24903
D. melanogaster: nompC-GAL4	Bloomington *Drosophila* Stock Center	BDSC: 36361; RRID: BDSC_36361
D. melanogaster:20XUAS-IVS-mCD8::GFP (attP2)	Bloomington *Drosophila* Stock Center	BDSC: 32194; RRID: BDSC_32194
D. melanogaster: UAS-GtACR1.d.EYFP (attP2)	Bloomington *Drosophila* Stock Center	BDSC: 92983; RRID: BDSC_92983
D. melanogaster: 10XUAS-IVS-mCD8::RFP (attP18) 13XLexAop2-mCD8::GFP (attP8)	Bloomington *Drosophila* Stock Center	BDSC: 32229; RRID: BDSC_ 32229
D. melanogaster: UAS-piezo.GFP	Bloomington *Drosophila* Stock Center	BDSC: 58773; RRID: BDSC_58773
D. melanogaster: fru-GAL4	A gift from Dr. Barry Dickson	N/A
D. melanogaster: fru-LexA	A gift from Dr. Bruce S. Baker	N/A
Software and algorithms		
Fiji software	https://fiji.sc	RRID:SCR_002285
DeepLabCut	https://github.com/DeepLabCut/DeepLabCut	N/A
Source code and data	https://github.com/HMYamano/piezo_copulation_source_code	https://doi.org/10.5281/zenodo.7780536

RESOURCE AVAILABILITY

Lead contact

Further information and requests for resources and reagents should be directed to, and will be fulfilled by, the lead contact: Azusa KAMIKOUCHI, kamikouchi.azusa.r4@f.mail.nagoya-u.ac.jp.

Materials availability

This study did not generate new unique reagents.

Data and code availability

- DeepLabCut models and training data have been deposited at Zenodo and are publicly available as of the date of publication. The DOI is listed in the key resources table. Any additional original/source data are available from the lead contact on request.

- All original code has been deposited at Zenodo and is publicly available as of the date of publication. The DOI is listed in the key resources table.
- Any additional information required to reanalyze the data reported in this paper is available from the lead contact upon request.

EXPERIMENTAL MODEL AND SUBJECT DETAILS

Fly strain

Fruit flies *D. melanogaster* were raised on standard yeast-based media at 25°C and 40% to 60% relative humidity on a 12 h light/12 h dark (12 h L/D) cycle. Canton-S (Hotta-lab strain, a gift from K. Ito) was used as a wild-type strain. w^{1118} was obtained from the Vienna *Drosophila* Resource Center. $piezo^{KO}$[32], *piezo-GAL4 (chr 3)*[32], *piezo-GAL4 (chr 2)*[32], *iav-GAL4, nan-GAL4 , nompC-GAL4, 20XUAS-IVS-mCD8::GFP (attP2), UAS-GtACR1.d.EYFP* (attP2),[50] *10XUAS-IVS-mCD8::RFP (attP18), 13XLexAop2-mCD8::GFP (attP8)*[61], *UAS-piezo.GFP*[32] were obtained from the Bloomington Drosophila Stock Center. fru-GAL4 was a kind gift from Dr. B. Dickson. fru-LexA was a kind gift from Dr. B. S. Baker.

For behavioral experiments, adult flies were maintained at 25°C under a 12 h L/D cycle. They were transferred to new tubes every 2 to 3 days, but not on the day of experiment. Wild-type adult females were used as mating partners. Both sexes of flies were collected within 8 h after eclosion to ensure their virgin status. Male flies were kept singly in a plastic tube (1.5 mL, Eppendorf) containing ~200 μL fly food. Females were kept in groups of 10 to 30. Males and females 5 to 8 days after eclosion were used for experiments. Males and females were used only once. All experiments were performed between Zeitgeber Time 1-11 at 25 ± 1°C and 50 ± 10% relative humidity.

For immunolabeling, males 5-10 days after eclosion were used.

METHOD DETAILS

Dissection and immunolabeling

Male genitalia were dissected in phosphate-buffered saline (PBS: Takara Bio Inc., #T900; pH 7.4 at 25°C), kept in 50% Vectashield mounting medium (Vector Laboratories, #H-1000; RRID: AB_2336789) in deionized water for ~5 min, and mounted on glass slides (Matsunami Glass IND., LTD, Osaka, Japan) using Vectashield mounting medium. Male forelegs and heads were dissected in PBS (pH 7.4 at 25°C), kept in 50% glycerol in PBS for ~5 min, and mounted with 80% glycerol in deionized water. Male internal genitalia were dissected in PBS (pH 7.4 at 25°C), fixed with 4% paraformaldehyde for 15 min at 25ºC, kept in 50% glycerol in PBS for ~10 min, and mounted with 80% glycerol in deionized water containing 1% DAPI (Sigma-Aldrich, # D9542).

Immunolabeling of the brains was performed as described previously with minor modifications.[62] Briefly, brains were dissected in PBS (pH 7.4 at 25ºC), fixed with 4% paraformaldehyde for 60-90 min at 4ºC, and subjected to antibody labeling. Brains were kept in 50% glycerol in PBS for ~1 h, 80% glycerol in deionized water for ~30 min, and then mounted. Rabbit polyclonal anti-GFP (Invitrogen, #A11122; RRID: AB_221569; 1:1000 dilution) was used for detecting the mCD8::GFP. Mouse anti-Bruchpilot nc82 (Developmental Studies Hybridoma Bank, #nc82, RRID:AB_2314866; 1:20 dilution) was used to visualize neuropils in the brain. Secondary antibodies used in this study were as follows: Alexa Fluor 488-conjugated anti-rabbit IgG (Invitrogen, #A11034; RRID:AB_2576217; 1:300 dilution) and Alexa Fluor 647-conjugated anti-mouse IgG (Invitrogen, #A21236; RRID: AB_2535805; 1:300 dilution).

Confocal microscopy and image processing

Serial optical sections were obtained at 0.84 μm intervals with a resolution of 512 × 512 or 1024 × 1024 pixels using an FV1200 or FV3000 laser-scanning confocal microscope (Olympus) equipped with a silicone-oil-immersion 30× (UPLSAPO30XSIR, NA = 1.05; Olympus) or 60× Super Apochromat objective lens (UPLSAPO60XS2, NA = 1.30; Olympus). The size, contrast, and brightness of the images were adjusted using Fiji software (version 2.3.0; RRID: SCR_002285).

Video recordings

We used CMOS cameras equipped with a 50 mm focal length lens (MVL50M23, Thorlabs, Inc. or VS-5026VM, VS Technology Corporation) for all experiments. The cameras used to record the fly behavior

in each assay are as follows: DFK 33UP1300 (The Imaging Source Asia Co., Ltd) in the copulation assay; DMK33UX273 (The Imaging Source Asia Co., Ltd.) equipped with a light-absorbing and infrared transmitting filter (IR-82, FUJIFILM) in the optogenetic assays. To time-stamp photostimulations, we used additional cameras as follows: DFK 33UP1300 (The Imaging Source Asia Co., Ltd.) for optogenetics using light emitting diode (LED); DFK 33UP1300 (2 sets; The Imaging Source Asia Co., Ltd.) for optogenetics using a laser. All recordings were performed at a resolution of 640 by 480 pixels and 30 frames/sec.

Copulation assays

Male homozygous *piezo*^{KO} mutants, heterozygous *piezo*^{KO} mutants, or wild-type flies were used. A round courtship chamber (10 mm diameter and 4 mm deep) enclosed with a slide glass and an acrylic plate as a lid and bottom, respectively, was used. A pair of male and female flies was introduced into the chamber by gentle aspiration without anesthesia.

After the video recording, we collected copulated females. Each female was kept in a plastic vial with food for 7 days and then removed. The number of pupae in each vial was counted 10 or 11 days after copulation.

Copulation disturbance assays

A pair of male and female flies were introduced into a 2 mL plastic tube by gentle aspiration without anesthesia. To facilitate copulation, we narrowed the space in the tube by inserting a 3D-printed plug into the tube until copulation (Figure S12). Tubes were monitored to identify the copulation initiation. When the copulation was initiated, we capped the tube and wrapped it with tape (1.5 mm width and ~80 mm length). 5 min after copulation initiation, we shook the tube for 30 s using a microtube mixer (MT-360, TOMY SEIKO CO. LTD.) at a frequency of ~38 Hz.

Creation of the DeepLabCut models

DeepLabCut,[43] the network model pretrained on the ResNet50, was used to detect male copulation posture automatically. We created four DeepLabCut models as follows: male copulation posture, copulation detection for LED, copulation detection for laser, and male copulation poster movement (See Table S2 for each training condition). In each training condition, movies were processed by Adobe Premiere Pro 2022 (Adobe Inc.) or VideoProc Converter (Chengdu Digiarty Software, Inc.) to collect the video clips of target events. We extracted images randomly from video clips and manually labeled the "keypoints" in each image (Figures S13A–S13C). To evaluate the performance of the trained DeepLabCut, we calculated the Root Mean Squared Error (RMSE), a measure to verify the goodness of the model, and confirmed that the pose predictions were sufficiently correct (Table S2).

Evaluation of male copulation posture

In all experiments, we defined copulation as a male mounting on a female for more than 1 min.[62,63] A custom-made Python script (version 3.8.13) was used for this evaluation. We collected the copulation video clips from the movie files on copulation assays using Adobe Premiere Pro 2022 (Adobe Inc.) or VideoProc Converter (Chengdu Digiarty Software, Inc.). We used the "male copulation posture model" of DeepLabCut to detect the wing bases of fly pairs in these video clips. Using coordinates of the wing bases, we defined the vectors $\overrightarrow{AB}$ and $\overrightarrow{CD}$, where *A*, *B*, *C*, and *D* correspond to the coordinates of the male-left, male-right, female-left, and female-right wing bases, respectively (Figure S14A). The vectors $\overrightarrow{AB}$ and $\overrightarrow{CD}$ are perpendicular to the body axes of the male and female, respectively, and thus were used to obtain the copulation angle, which represents the angle between the body axes (Figure S14A; note that the angle between these two vectors is equivalent to the copulation angle).[64] In this analysis, we used the frames in which all the keypoints on the wing bases showed $\geq$ 0.9 likelihood. We used movie files to compare the data when the total duration of the calculated frames was at least 5 min, to avoid large discrepancies between the actual value and the calculated value due to the short observation duration (Figures 2C and 2D). The total frame numbers that were analyzed in *Piezo*^{KO} groups were not significantly different from that in heterozygous (*Piezo*^{KO}/+) control groups (Figure S14B). The ratio of time in which the male engaged in tilted copulation was significantly larger in *Piezo*^{KO} homozygous males than in control flies even when the threshold of copulation angle to define the tilted copulation was changed between 20° and 30° (Figures S2A–S2K).

In optogenetic assays using a laser, the male copulation position was defined by the middle point of wing bases, $\overline{w}$, during copulation. The movement of the male copulation position during photostimulation was quantified as the difference of the copulation position coordinate from the previous frame (1 mm = 40.36 ± 0.17 pixels). The average displacement of the male copulation position per second was obtained by:

$$Dt \,/\, Time$$

where *Dt* is the cumulative displacement of the male copulation position during the observation time (*Time*), which was defined as follows:

(1) For pairs that continued copulation during photostimulation, we set their observation time as the duration of photostimulation.

(2) For pairs that terminated copulation during photostimulation, we ended their observation time at the time of copulation termination.

In optogenetic assays using LEDs, we did not assess the male copulation position because the movement of the anterior body (especially due to head grooming) during photostimulation induced a large fluctuation of the male copulation position.

Optogenetic assays – retinal feeding

Males of *piezo>GtACR1* flies were maintained under a dark condition for 4 to 6 days after eclosion and then transferred to a plastic tube (1.5 mL, Eppendorf) containing ~150μL of fly food. Plastic tubes that contain males were divided into two groups: experimental and control groups. For the experimental group, 2 μL of all trans-retinal (R2500, Sigma-Aldrich), 25mg/mL dissolved in 99.5% ethanol (14033-80, KANTO KAGAKU), was placed on the food surface. For the control group, 2 μL of 99.5% ethanol was placed instead. All trans-retinal is a light-sensitive pigment that enables the triggering of ion flux through green-light absorption. The male flies were kept on each food for 24 to 36 h before being used for the assays.

Optogenetic assays - fixing females

We used a piece of eraser (~2 mm length, ~1 mm width, and ~0.5 mm height) as the copulation stage, which was fixed at the center of a slide glass using light-curing adhesives (1771E, ThreeBond Holdings Co., Ltd.). Each female was anesthetized on ice for ~30 sec and glued to the eraser using the light-curing adhesives. Males were introduced after the recovery of females. In all optogenetic assays, we used glued females.

Optogenetic assays - photostimulation

A courtship chamber (10-mm diameter and 4-mm height for LED photostimulation; 10 mm x 10 mm x 4 mm with an 1 mm fillet radius for laser photostimulation) made of an aluminum plate with an anodic oxide coating to prevent light reflection, was used. The chamber was illuminated from above by an infrared LED ring light (FRS5CS, 850 nm, OptoSupply) to enable recordings in dark conditions. A female attached to the copulation stage was placed in the center of the courtship chamber. After the recovery of females from anesthesia, a male fly was gently aspirated into the chamber without anesthesia and sealed with a cover glass (Matsunami Glass IND., LTD, Osaka, Japan).

We used a custom script for Bonsai,[65] a visual programing language, to detect the copulation initiation. Five min after the copulation was initiated, we started photostimulation using LED or laser. We set the intensity of the photostimulation in the same intensity range used in a previous study.[50] For photostimulation with LEDs, a 525 nm LED (OSG5XNE3E1E, OptoSupply) was applied for 30 sec from the bottom of the chamber at the intensity of 5.8 mW/cm^2 and 30 Hz with a duty ratio of 0.2. In the assay using laser, a 532 nm laser light (JPM-1-3, Lightvision Technologies, Corp.) was applied for 30 sec near male genitalia from the left or right side of the body at the intensity of 5.6 mW/cm^2 and 30 Hz with a duty ratio of 0.5. The light intensity of photostimulation was calibrated with a photometer (PM100D, Thorlabs, Inc.).

In optogenetic assays with a laser, we saved a snapshot of the illumination area from the side camera video, at the first frame after light intensity saturated (~0.5 sec after the laser onset). We measured the laser focusing point (the center of the photostimulation area assuming that all photostimulation areas are of uniform value) using Fiji software (version 2.3.0; RRID: SCR_002285). We confirmed in all videos that the area of

the laser diameters, defined by the laser profiling, from the center of gravity of the photostimulation did not include the thorax of a male fly.

Optogenetic assays – laser profiling

We evaluated the laser beam diameter used in optogenetic assays to ascertain the area of photostimulation. A laser beam profiler (Beamage-3.0, Gentec-EO) was used to measure the laser light intensity distribution at 23°C (Figures S9A and S9B). From the intensity distribution data, we calculated the beam diameter as 1.639 mm. The laser diameter was defined as the distance between two points equal to $1/e^2$ times the maximum intensity. Outside of the laser diameter, the laser intensity was too low to activate GtACR1 channels.[50] R (version 4.2.1) and Python (version 3.8.13) were used.

Optogenetic assays - A closed-loop system

We used a desktop PC equipped with NVIDIA GeForce RTX 2080 as GPU (OS, Windows 10; CPU, Intel Core i7-9700K; RAM, 32 GB). The program scripts were written by Bonsai.[65] We adopted the trained DeepLabCut models (copulation detection models for LED and laser, respectively) for the DeepLabCut-Live![66] to track the keypoints on flies online during video recordings. We then obtained the coordinate of the middle point of wing bases, $\overline{w}$, as well as that of eyes, $\overline{e}$, to detect the copulation event. To detect copulation events, two distance values were used: (1) the distance between the female $\overline{w}$ and male $\overline{e}$, and (2) the distance between the male $\overline{w}$ and the female scutellums (Figure S14C). Copulation was judged positive when both values were less than or equal to $20\sqrt{10}$pixel ($\cong$1.6 mm; 1 mm = 40.73 $\pm$ 0.25 pixel), which was determined by measuring the distances in the five video clips of the training dataset.

With this threshold value, no false negatives were detected. False positives were detected, however, and thus we set an additional criterion that uses three checkpoints (2, 5, and 15 sec after the first copulation detection) to reduce the false positives; only when it judged the image as positive at all three checkpoints, the system accepted it as the copulation event. In this step, we used a custom Arduino script.

We used Arduino IDE (version 1.8.19, Arduino) written on a microcomputer AE-ATMEGA-UNO-R3 (Base on Arduino UNO; AKIZUKI DENSHI TSUSHO CO., LTD.) to turn on the LED upon receiving a trigger signal from the custom Bonsai scripts that had detected the copulation event. See Table S3 for a list of false negatives and false positives that indicates the evaluation of each DeepLabCut-Live! Model.

Manual behavior analysis

For copulation rate analysis (Figure 3C), we calculated the ratio of pairs showing copulation success. We defined copulation success as maintenance of male and female genital coupling for longer than 30 sec. For female kicking analysis (Figure S3A), we divided each movie file into 1-sec bins and counted the number of bins that contained the event of female kicking the male with her hind legs during copulation. The ratio of event-positive bins per total bins that cover the entire copulation period was calculated. For genitalia touching analysis (Figure S3B), we measured the number of time male genitalia touched female genitalia when the male performed abdominal bending prior to copulation success. The number of genitalia touching was normalized by the latency to copulation initiation.

Locomotor activity analysis

Male locomotor activity was quantified using the *Drosophila* activity monitoring system (Trikinetics Inc). Each male was introduced into a glass tube (5 × 65mm) with standard yeast-based media. After acclimation to the new environment overnight, locomotor activity was measured for 10h (ZT1-11). Locomotor activity data was collected in 1-min bins, and the number of the beam-breaks was analyzed.

QUANTIFICATION AND STATISTICAL ANALYSIS

Statistical analyses were conducted using R (version 4.2.1) and Python (version 3.8.13). Aligned rank transform one-way analysis of variance (ART one-way ANOVA) and Brunner–Munzel tests were used for comparisons between conditions after verifying the equality of variance (Bartlett's test for three-groups comparisons; F-tests for two-groups comparisons) and normality of the values (Shapiro-Wilk test) (Table S4). For the ART one-way ANOVA, the ARTool package (version 0.11.1) was used (https://github.com/mjskay/ARTool/).[67,68] After ART one-way ANOVA, p values were adjusted using the Benjamini-Hochberg method in the post hoc test. For the Brunner-Munzel test, the brunnermunzel package (version

1.4.1) was used (https://github.com/toshi-ara/brunnermunzel). The statistical methods and values are summarized in Table S5. Statistical significance was set at $p < 0.05$. Boxplots were drawn using the R package ggplot2 (https://ggplot2.tidyverse.org/). Boxplots represent the median and interquartile range (the distance between the first and third quartiles), and whiskers denote 1.5 × the interquartile range. The statistical methods and results in this study are summarized in Table S5.